

IMPROVED FLAT-BACK 3D GADGETS IN ORIGAMI EXTRUSIONS COMPLETELY DOWNWARD COMPATIBLE WITH THE CONVENTIONAL PYRAMID-SUPPORTED 3D GADGETS

MAMORU DOI

Abstract. An origami extrusion is a folding of a 3D object in the middle of a flat piece of paper, using 3D gadgets which create faces with solid angles. In this paper we focus on 3D gadgets which create a top face parallel to the ambient paper and two side faces sharing a ridge, with two outgoing simple pleats, where a simple pleat is a pair of a mountain fold and a valley fold. There are two such types of 3D gadgets. One is the conventional type of 3D gadgets with a triangular pyramid supporting the two side faces from inside. The other is the newer type of 3D gadgets presented in our previous paper, which improve the conventional ones in several respects: They have flat back sides above the ambient paper and no gap between the side faces; they are less interfering with adjacent gadgets so that we can make the extrusion higher at one time; they are downward compatible with conventional ones if constructible; they have a modified flat-back gadget used for repetition which does not interfere with adjacent gadgets; the angles of their outgoing pleats can be changed under certain conditions. However, there are cases where we can apply the conventional gadgets while we cannot our previous ones. The purpose of this paper is to improve our previous 3D gadgets to be completely downward compatible with the conventional ones, in the sense that any conventional gadget can be replaced by our improved one with the same outgoing pleats, but the converse is not always possible. To be more precise, we prove that for any given conventional 3D gadget there are an infinite number of improved 3D gadgets which are compatible with it, and the conventional 3D gadget can be replaced with any of these 3D gadgets without affecting any other conventional 3D gadget. Also, we see that our improved 3D gadget keep all of the above advantages over the conventional ones.

1. INTRODUCTION

An *origami extrusion* is a folding of a 3D object in the middle of a flat piece of paper, with the paper around the 3D object kept flat. The mechanisms in origami extrusions which create faces with solid angles are called *3D gadgets*.

In general, to construct such a 3D gadget we begin with its development, which is a flat piece of paper with a net of the faces of the extruded object on it. Also, we prescribe the creases of some pleats going out of the extruded object (which we call *outgoing pleats*) by which we ‘inflate’ the paper, and then design the rest of the creases in the region which is hidden behind after the folding. Thus given a net of a 3D object and prescribed creases of outgoing pleats, we may have more than one way of making an extrusion with the same appearance. If two 3D gadgets have the same net of the extruded object and prescribed creases of outgoing pleats, then they are compatible if we ignore other 3D gadgets. However, in the presence of other 3D gadgets, even if the replacement of one gadget (say gadget A) with the other (say gadget B) is possible, the converse replacement (of gadget B with gadget A) may not because gadget A may collide with other gadgets. In such a case we say that gadget B is *downward compatible* with gadget A.

This paper is a sequel to our previous paper [1], and we focus on 3D gadgets which create a top face parallel to the ambient paper and two side faces sharing a ridge, with two outgoing simple pleats, where a simple pleat is a pair of a mountain fold and a valley fold. There are two known types of such 3D gadgets. The older is that of the conventional pyramid-supported gadgets. For

example, in the crease pattern (also abbreviated as ‘CP’) of the conventional cube gadget shown in Figure 1.1, the shadowed part (being a square for the cube gadget but a hexagon in general) forms a triangular pyramid and supports the side faces from inside in the resulting extrusion as in Figure 1.3. The newer is that of the flat-back gadgets which we presented in the previous paper. For example, in the crease pattern of our new cube gadget in Figure 1.2, the pleats formed by the upper left and right shadowed kites, which we call ‘ears’ in [1], support the side faces, and the pleat formed by the lower kite, which we call a ‘tongue’ lies in the bottom plane and thrusts inside the angle between the side faces in the resulting extrusion as in Figure 1.4.

Our 3D gadgets presented in our previous paper have several advantages over the conventional ones as follows:

- They have flat back sides above the ambient paper, which enables us to make origami extrusions being flat-foldable or having curved creases. Also, they have no gap between the side faces, which makes the appearance better, while the conventional ones have a gap from which we can see the inside space bounded by the faces of the supporting pyramid.
- They are less interfering with adjacent 3D gadgets. Thus we can make the extrusion higher at one time.
- We can easily change the angles of the outgoing pleats of our 3D gadgets under certain conditions, which is impossible or at least difficult for the conventional ones.
- If our 3D gadget is compatible with a conventional one, it is also downward compatible.
- There are modified flat-back 3D gadgets used for repeating or dividing our 3D gadgets, which have a good property that they do not interfere with other gadgets.

Note that the fourth item does not say that there always exists a 3D gadget of ours which is compatible with a given conventional one. For example, if a conventional 3D gadget has a side face with inner angle less than or equal to $\pi/4$ at the point where the top and the side faces assemble, we cannot construct a 3D gadget of ours compatible with it. This is one of the few inferior points of our previous 3D gadgets to the conventional ones. We show in Figure 2.2 an example of the crease pattern of such a conventional 3D gadget, where $\beta_L = \pi/4$.

The purpose of this paper is to improve our 3D gadgets to be *completely downward compatible* with the conventional pyramid-supported ones. To be more precise, we prove that for any given conventional 3D gadget there are an infinite number of improved 3D gadgets which are compatible with it, and the conventional 3D gadget can be replaced with any of these 3D gadgets without affecting any other conventional 3D gadget. Also, we see that our improved 3D gadgets keep all of the above advantages over the conventional ones.

To explain the main idea to achieve this end, we consider the crease pattern as given in Figure 1.5. In this crease pattern, creases ℓ_σ, m_σ for $\sigma = L, R$ are prescribed so that the resulting gadget is compatible with a conventional one, and C is determined as the point to which B_L and B_R swing. However, since D is a point such that segments AB_L and AB_R swing to overlap with segment AD , it is necessary for D to lie on the circular arc $B_L B_R$ with center A , but not on segment AC . Indeed, we see in Figure 1.5 that as we move point D on the circular arc $B_L B_R$, the shadowed kites forming the ears and the tongue deform correspondingly, so that the crease pattern gives another cube gadget. Thus $\phi_\sigma = \angle B_\sigma AD$ parametrizes the deformations of the gadget. This is the main starting idea of this paper.

In this paper, we will consider a condition (4.3) for the construction of our improved 3D gadget to be possible in terms of $\angle AB_\sigma E_\sigma$ for $\sigma = L, R$ in Figure 1.5. However, since condition (4.3) cannot be checked a priori, we rewrite it in terms of $\phi_\sigma = \angle B_\sigma AD$ to obtain a condition (4.5) which is geometrically easy to check and gives a construction of our improved gadgets (Construction 3.7). Then we further rewrite it in terms of $\psi_\sigma = \angle B_\sigma AC - \angle B_\sigma AD$ to obtain another condition (4.13), which is a natural extension of the condition obtained in [1]. Also, we prove in Theorem 4.6 that there always exists ψ_L and ψ_R which satisfy (4.13) for $\sigma = L, R$ without additional conditions. Lastly,

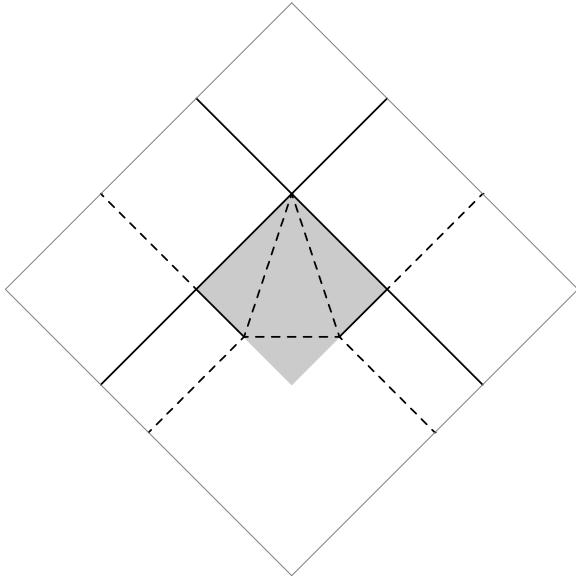


FIGURE 1.1. CP of the conventional cube gadgets

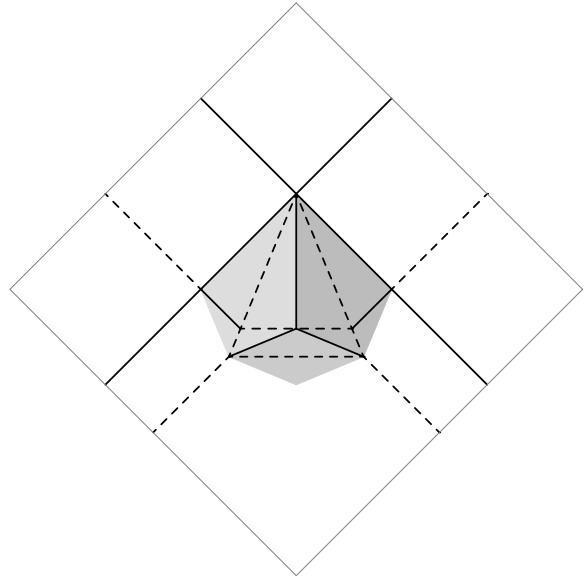


FIGURE 1.2. CP of our new cube gadget

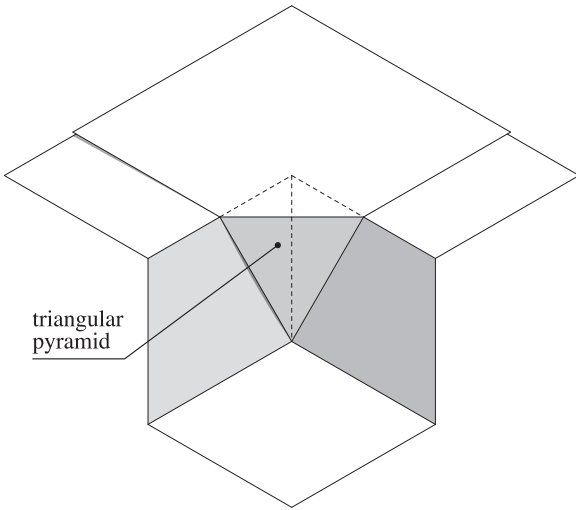


FIGURE 1.3. Back view of the conventional cube gadgets

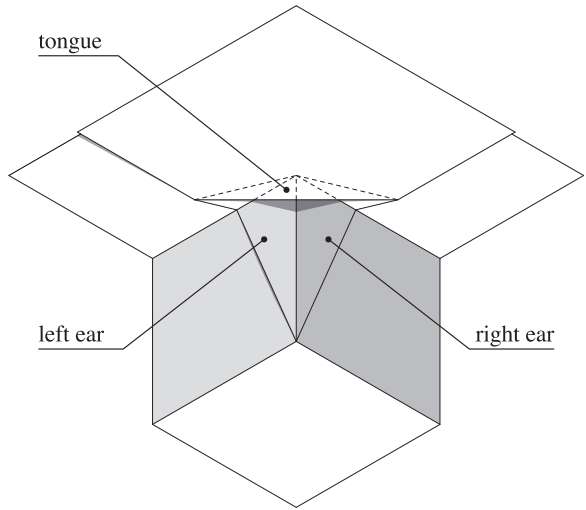


FIGURE 1.4. Back view of our new cube gadget

we obtain another equivalent condition (6.3) in terms of $\epsilon_\sigma = \angle E_\sigma D G_\sigma$ (its general definition is given by (6.1)), which gives an alternative construction of our gadgets (Construction 6.2).

This paper is organized as follows. Section 2 recalls the construction of the conventional pyramid-supported 3D gadgets and check that the construction is indeed possible under the given conditions. Section 3 gives the construction of our improved 3D gadgets. To determine the range of $\phi_\sigma = \angle B_\sigma A D$ in the construction, we introduce *critical angles* and impose a condition which the critical angles must satisfy. In Section 4 we discuss the validity of the conditions given in the construction of the improved 3D gadgets in Section 3. We also check the constructibility and the foldability of the crease pattern. For this purpose, we give the constructibility condition in two ways (Theorems 4.1 and 4.3), where the latter gives a natural extension of [1]. Furthermore, we prove in

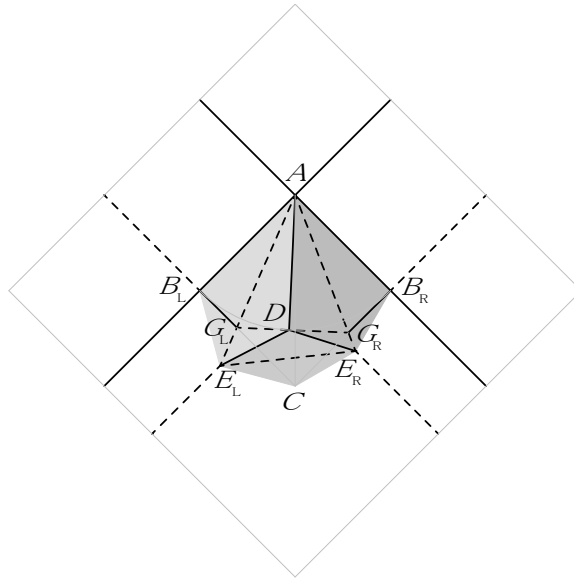


FIGURE 1.5. CP of a deformation of our new cube gadget

two ways that the above condition we imposed on the critical angles in Section 3 always holds, and thus can be removed (Theorem 4.6). In Section 5 we recall the interference coefficients introduced in our previous paper, and calculate those of the improved 3D gadgets compatible with a given conventional one, all of which are proved to be less than or at worst equal to those of the conventional one. This result and Theorem 4.6 together prove the downward compatibility of our improved 3D gadgets with the conventional ones (Theorem 5.3). In Section 6 we give some useful gadgets for typical choices of ϕ_σ among infinite possible choices. Also, we give an alternative construction of our 3D gadgets specifying certain angles. Then we study some examples of our improved 3D gadgets. Section 7 gives the construction of flat-back 3D gadgets which are used to repeat our improved gadgets and make the extrusion higher with the same interference distances. Section 8 gives our conclusion.

Details of the background of this research and our settings are explained in our previous paper, and we will not repeat them here.

Notation and terminology. To keep consistency with the previous paper, we will use the same notation and terminology as possible as we can. One exception is the use of ϕ_σ , which is defined to be $\phi_\sigma = \beta_\sigma + \gamma_\sigma/2 - \pi/2$ in the previous paper, while $\phi_\sigma = \angle B_\sigma AD$ in the present paper.

We use subscript σ for L and R which stand for ‘left’ and ‘right’ respectively. Also, we use subscript σ' to indicate the other side of σ , that is,

$$\sigma' = \begin{cases} \text{R} & \text{if } \sigma = \text{L}, \\ \text{L} & \text{if } \sigma = \text{R}. \end{cases}$$

2. THE CONVENTIONAL PYRAMID-SUPPORTED 3D GADGETS DEVELOPED BY NATAN

Before constructing our improved 3D gadgets, let us recall the construction of the conventional pyramid-supported 3D gadgets, which was developed by Carlos Natan [3] as a generalization of the conventional cube gadget shown in Figure 1.1. We consider the following local model as in [1].

- (A) The object we want to extrude in the middle of the paper (which we suppose to be in the xy -plane $H_0 = \{z = 0\}$) with a 3D gadget is a part of a polyhedron such that its top face is bounded by two rays j_L and j_R starting from A in $H_h = \{z = h\}$, and its bottom face is bounded by two rays k_L and k_R with k_σ parallel to j_σ for $\sigma = \text{L}, \text{R}$, starting from B in

$H_0 = \{z = 0\}$. Suppose the inner angle α of the top face at A (and so the inner angle of the bottom face at B) satisfies $0 < \alpha < \pi$.

(B) There are only simple pleats outside the extruded object.

Let $\beta_\sigma = \angle BAj_\sigma = \pi - \angle ABk_\sigma$ for $\sigma = L, R$ and $\gamma = 2\pi - \alpha - \beta_L - \beta_R$. Then we develop the top and side faces on the paper as in Figure 2.1, where ℓ_L and ℓ_R are the mountain folds of the outgoing pleats, and AB_L and AB_R assemble to form ridge AB . The construction of the conventional pyramid-supported 3D gadgets are given as follows.

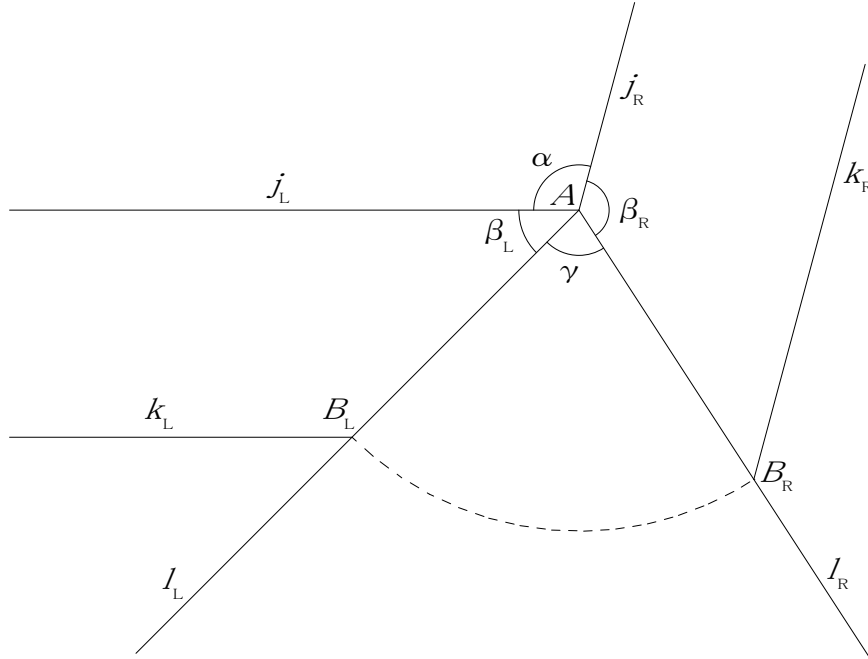


FIGURE 2.1. Development to which we apply a conventional 3D gadget

Construction 2.2. Consider a development as shown in Figure 2.1, for which we require the following conditions. (Here we use the term ‘development’ instead of ‘net’ to indicate that the piece of paper we consider includes not only a net of the extruded object, but also prescribed creases and regions which are hidden behind after the folding.)

- (i) $\alpha < \beta_L + \beta_R$, $\beta_L < \alpha + \beta_R$ and $\beta_R < \alpha + \beta_L$.
- (ii) $\alpha + \beta_L + \beta_R < 2\pi$.
- (iii) $\alpha + \beta_L + \beta_R > \pi$.

Then the crease pattern of the pyramid-supported 3D gadget is constructed as follows, where all procedures are done for both $\sigma = L, R$.

- (1) Draw a perpendicular to ℓ_σ through B_σ for both $\sigma = L, R$, letting C be the intersection point.
- (2) Draw a perpendicular bisector m_σ to segment $B_\sigma C$.
- (3) Determine a point D_σ on m_σ such that $\angle AB_\sigma D_\sigma = \pi - \beta_\sigma$, and restrict m_σ to a ray starting from D_σ and going in the same direction as ℓ_σ .
- (4) The desired crease pattern is shown as the solid lines in Figure 2.3, and the assignment of mountain folds and valley folds is given in Table 2.4.

In the rest of this section, we check that Construction 2.2 of the conventional pyramid-supported 3D gadgets is possible under conditions (i)–(iii).

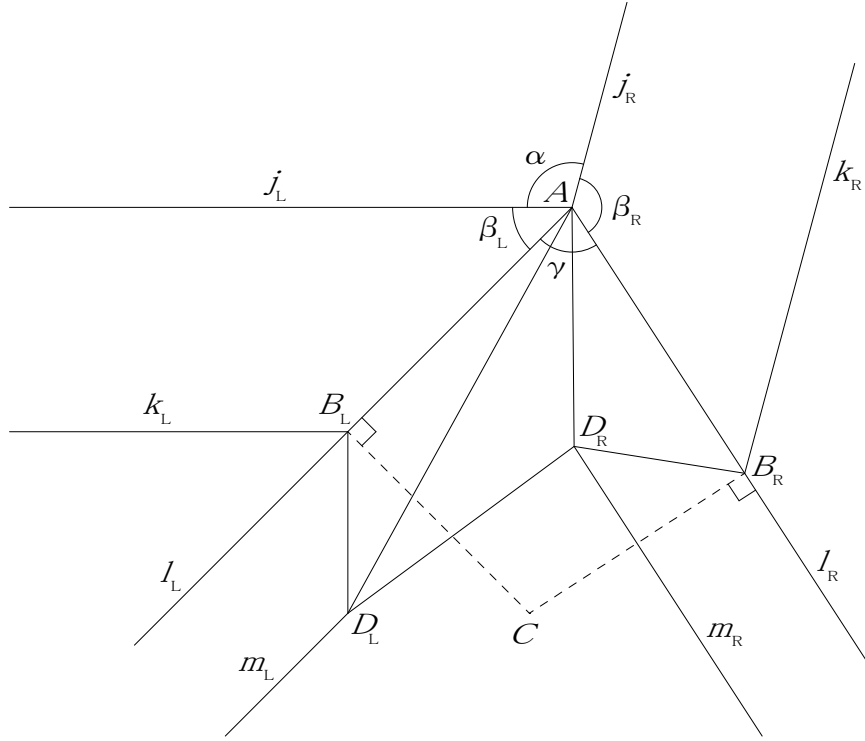


FIGURE 2.3. CP of the conventional 3D gadget

mountain folds	$j_\sigma, \ell_\sigma, AB_\sigma, B_\sigma D_\sigma$
valley folds	$k_\sigma, m_\sigma, AD_\sigma, D_L D_R$

TABLE 2.4. Assignment of mountain folds and valley folds to the conventional 3D gadget

From conditions (i) and (ii), we see that $\alpha < \pi$ and

$$(2.1) \quad \beta_\sigma + \gamma/2 < \pi \quad \text{for } \sigma = L, R.$$

Also, condition (iii) ensures that point C exists inside $\angle B_L A B_R = \gamma$.

Let P be the intersection point of the extensions of m_L and m_R . Then since P is the excenter of $\triangle B_L B_R C$, AP is a perpendicular bisector of $B_L B_R$ (see also Lemma 3.5). Thus it follows from (2.1) that

$$\angle AB_\sigma P = \gamma/2 < \pi - \beta_\sigma = \angle AB_\sigma D_\sigma \quad \text{for } \sigma = L, R,$$

which implies that points D_L and D_R in procedure (3) exist and segment AD_L is located to the left of segment AD_R .

Now we check that triangles $\triangle AB_L D_L$, $\triangle AB_R D_R$, $\triangle AD_L D_R$ and $\triangle CD_L D_R$ form a triangular pyramid. As B_L and B_R swing to C , AB_L , $B_L D_L$ and $B_R D_R$ glue to AB_R , CD_L and CD_R of the same lengths respectively. Also, $\angle AB_L D_L$, $\angle AB_R D_R$ and $\angle D_L C D_R$ form a solid angle around vertex C because we have

$$\angle AB_L D_L + \angle AB_R D_R + \angle D_L C D_R = (\pi - \beta_L) + (\pi - \beta_R) + \alpha = 2\pi - (\beta_L + \beta_R - \alpha) < 2\pi$$

by condition (i). The sums of angles which assemble at other vertices A , D_L and D_R are obviously less than 2π respectively. Hence hexagon $AB_L D_L C D_R B_R$ with creases AD_L , AD_R and $D_L D_R$ is a net of triangular pyramid $ACD_L D_R$, which fits and supports the side faces $j_\sigma AB_\sigma k_\sigma$ for $\sigma = L, R$

from inside. Flat-foldability of the region below polygonal chain $k_L B_L D_L D_R B_R k_R$ is obvious. Hence Constuction 2.2 is possible under conditions (i)–(iii).

Note that the existence of the triangular pyramid $ACD_L D_R$ implies that

$$(2.2) \quad \angle B_L A D_L + \angle B_R A D_R > \angle D_L A D_R,$$

which will be crucial in constucting our improved 3D gadgets.

3. CONSTRUCTION OF IMPROVED FLAT-BACK 3D GADGETS

We begin with the following definition, which will be needed in the construction of our improved flat-back 3D gadgets.

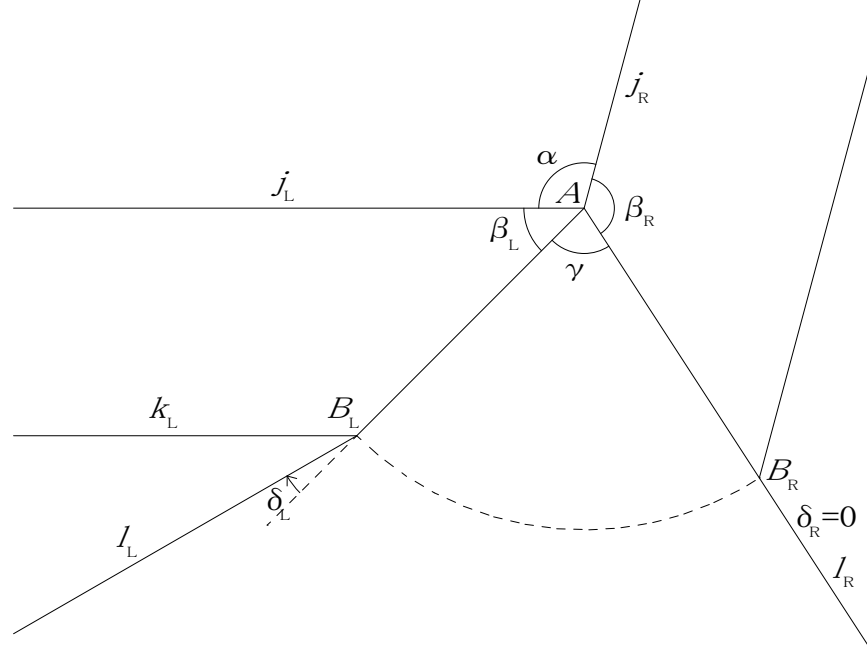


FIGURE 3.1. Development to which we apply our flat-back 3D gadget

Definition 3.2. Consider a development as in Figure 3.1, which is different from Figure 2.1 in that we allow changes $\delta_\sigma > 0$ of angles of the outgoing pleats. We require the following conditions.

- (i) $\alpha < \beta_L + \beta_R$, $\beta_L < \alpha + \beta_R$ and $\beta_R < \alpha + \beta_L$.
- (ii) $\alpha + \beta_L + \beta_R < 2\pi$.
- (iii.a) $\delta_L, \delta_R \geq 0$, where we take clockwise (resp. counterclockwise) direction as positive for $\sigma = L$ (resp. $\sigma = R$).
- (iii.b) $\delta_\sigma < \beta_\sigma$ and $\delta_\sigma < \pi/2$ for $\sigma = L, R$.
- (iii.c) $\alpha + \beta_L + \beta_R - \delta_L - \delta_R > \pi$, or equivalently, $\gamma + \delta_L + \delta_R < \pi$.

We define a *critical angle* ζ_σ for $\sigma = L, R$ with $0 < \zeta_\sigma \leq \gamma/2$ by the following construction, where all procedures are done for both $\sigma = L, R$.

- (1) Draw a perpendicular to ℓ_σ through B_σ for both $\sigma = L, R$, letting C be the intersection point.
- (2) Draw a perpendicular bisector m_σ to segment $B_\sigma C$.
- (3) Let P be the intersection point of m_L and m_R , and restrict m_σ to a ray starting from P and going in the same direction as ℓ_σ . Since P is the excenter of $\triangle C B_L B_R$, segment AP is a perpendicular bisector of segment $B_L B_R$ and also a bisector of $\angle B_L A B_R$.
- (4) Draw a ray n_σ starting from B_σ and going inside $\angle B_L A B_R$ so that $\angle A B_\sigma n_\sigma = \pi - \beta_\sigma + \delta_\sigma$.

(5) Let Q_σ be the intersection point of ray n_σ and polygonal chain APm_σ .

(6) Then we define ζ_σ by

$$(3.1) \quad \zeta_\sigma = \angle B_\sigma A Q_\sigma.$$

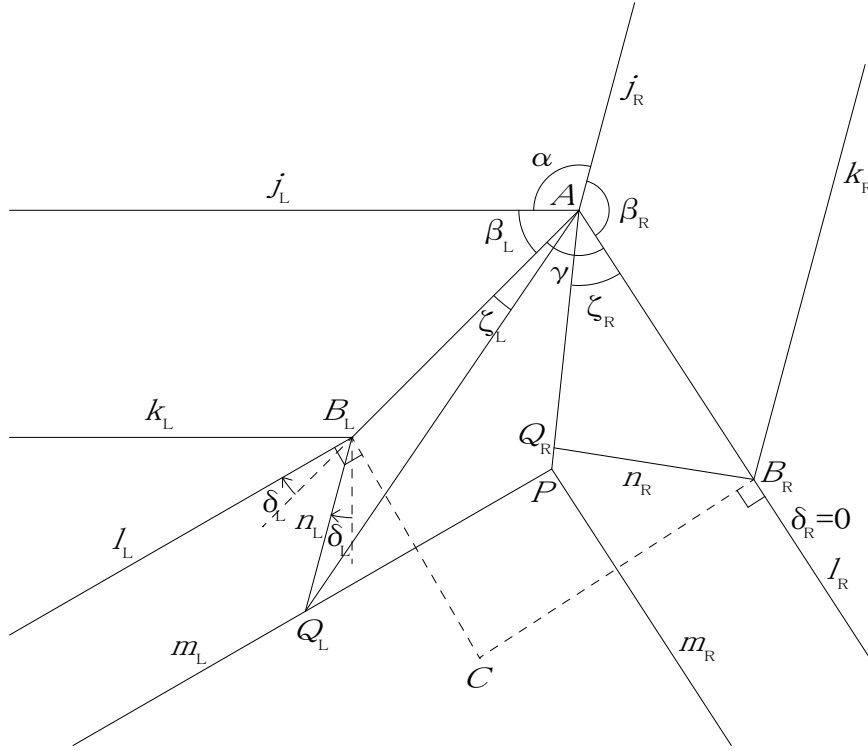


FIGURE 3.3. Construction of the critical angles ζ_L and ζ_R

Lemma 3.4. *Suppose $\delta_L = \delta_R = 0$ in Definition 3.2. Then Q_σ coincides with point D_σ in Construction 2.2. Also, we have $\zeta_L + \zeta_R > \gamma/2$.*

Proof. The first part is obvious from the constructions of Q_σ and D_σ . The second part follows immediately from (2.2). \square

Lemma 3.5. *In Definition 3.2 we have*

$$(3.2) \quad \begin{aligned} \angle AB_L P &= \angle AB_R P = \gamma/2 + \delta_L + \delta_R, \\ \angle PB_\sigma \ell_\sigma &= \pi - \gamma/2 - \delta_\sigma. \end{aligned}$$

Proof. Define angles μ and ν_σ by

$$\mu = \angle AB_L P - \angle AB_L B_R = \angle AB_R P - \angle AB_R B_L, \quad \nu_\sigma = \angle B_\sigma B_\sigma' C.$$

Then we see from the sum of the inner angles of $\triangle B_L B_R C$ with excenter P that

$$(3.3) \quad 2(\nu_L + \nu_R - \mu) = \pi.$$

Also, we have

$$(3.4) \quad \angle AB_\sigma B_\sigma' - \delta_\sigma + \nu_\sigma = \pi/2,$$

and thus putting $\angle AB_\sigma B_\sigma' = (\pi - \gamma)/2$ into (3.4) gives that

$$(3.5) \quad \nu_\sigma = \frac{\gamma}{2} + \delta_\sigma.$$

Combining (3.3) and (3.5), we get

$$\mu = \gamma + \delta_L + \delta_R - \frac{\pi}{2},$$

so that we have consequently

$$\angle AB_\sigma P = \angle AB_\sigma B_{\sigma'} + \mu = \frac{\pi - \gamma}{2} + \left(\gamma + \delta_L + \delta_R - \frac{\pi}{2} \right) = \frac{\gamma}{2} + \delta_L + \delta_R$$

as desired. The second expression of (3.2) is then immediate. This completes the proof of Lemma 3.5. \square

Proposition 3.6. *The critical angle ζ_σ in Definition 3.2 is given by*

$$(3.6) \quad \zeta_\sigma = \begin{cases} \tan^{-1} \left(\frac{1 - d_\sigma/c'}{1/c + 1/c' + (1 + d_\sigma/c)/b_\sigma} \right) & \text{if } \beta_\sigma + \gamma/2 + \delta_{\sigma'} \leq \pi, \\ \gamma/2 & \text{if } \beta_\sigma + \gamma/2 + \delta_{\sigma'} \geq \pi, \end{cases}$$

where we set

$$b_\sigma = \tan(\beta_\sigma - \delta_\sigma), \quad c = \tan(\gamma/2), \quad c' = \tan(\gamma/2 + \delta_L + \delta_R), \quad \text{and } d_\sigma = \tan \delta_\sigma.$$

In particular, if $\delta_L = \delta_R = 0$, then we have $c = c' = \tan(\gamma/2)$ and $d_L = d_R = 0$, so that

$$(3.7) \quad \zeta_\sigma = \tan^{-1} \left(\frac{1}{2/\tan(\gamma/2) + 1/\tan \beta_\sigma} \right) < \frac{\gamma}{2}.$$

Proof. First suppose $\angle AB_\sigma P \geq \angle AB_\sigma n_\sigma$ in Definition 3.2, (b), which is equivalent to $\beta_\sigma + \gamma/2 + \delta_{\sigma'} \geq \pi$ by Lemma 3.5. Then n_σ intersects segment AP at Q_σ , and thus we have $\zeta_\sigma = \gamma/2$ from Definition 3.2.

Next suppose $\beta_\sigma + \gamma/2 + \delta_{\sigma'} \leq \pi$. We may assume $\sigma = L$ and $A = (0, 0), B_L = (1, 0)$. Then P is written as

$$(3.8) \quad P = p(1, c) = (1, 0) + q(1, -c')$$

for some $p, q \in \mathbb{R}$. Solving (3.8), we get

$$(p, q) = \frac{1}{c + c'}(c', c), \quad P = \frac{c'}{c + c'}(1, c).$$

Furthermore, since Q_L is the intersection point of m_L with slope $-d_L$ and n_L with slope b_L , Q_L is written as

$$(3.9) \quad Q_L = \frac{c'}{c + c'}(1, c) + r(1, -d_L) = (1, 0) + s(1, b_L).$$

for some $r, s \in \mathbb{R}$. Solving (3.9), we get

$$(r, s) = \frac{c}{(b_L + d_L)(c + c')} (c' + b_L, c' - d_L),$$

so that

$$Q_L = \frac{1}{(b_L + d_L)(c + c')} (b_L(c + c') + (c + d_L)c', b_L c(c' - d_L)).$$

This gives that

$$(3.10) \quad \tan \zeta_L = \tan \angle B_L A Q_L = \frac{1 - d_L/c'}{1/c + 1/c' + (1 + d_L/c)/b_L}.$$

Since $0 < \zeta_L \leq \gamma/2 < \pi/2$, we obtain an expression of ζ_L for $\beta_L + \gamma/2 + \delta_R \leq \pi$ by taking the arc tangent of (3.10). Also, interchanging L and R gives ζ_R . \square

Now we construct our improved flat-back 3D gadget, which is compatible with the conventional one obtained in Construction 2.2 if $\delta_L = \delta_R = 0$.

Construction 3.7. Consider a development as in Figure 2.1, for which we require the following conditions.

- (i) $\alpha < \beta_L + \beta_R$, $\beta_L < \alpha + \beta_R$ and $\beta_R < \alpha + \beta_L$.
- (ii) $\alpha + \beta_L + \beta_R < 2\pi$.
- (iii.a) $\delta_L, \delta_R \geq 0$, where we take clockwise (resp. counterclockwise) direction as positive for $\sigma = L$ (resp. $\sigma = R$).
- (iii.b) $\delta_\sigma < \beta_\sigma$ and $\delta_\sigma < \pi/2$ for $\sigma = L, R$.
- (iii.c) $\alpha + \beta_L + \beta_R - \delta_L - \delta_R > \pi$, or equivalently, $\gamma + \delta_L + \delta_R < \pi$.
- (iv) $\zeta_L + \zeta_R \geq \gamma/2$, where ζ_σ is given by (3.1) or (3.6). (This condition is proved to be *unnecessary* in Theorem 4.6.)

Conditions (i)–(iii) are the same as in Construction 2.2 if $\delta_L = \delta_R = 0$, and the same as in Definition 3.2 and [1], Construction 3.2. By Lemma 3.4, Condition (iv) holds automatically for $\delta_L = \delta_R = 0$ if conditions (i)–(iii) hold. Therefore, our improved 3D gadgets is *completely compatible* with those in Construction 2.2. We discuss the validity of these conditions in Section 4.

The crease pattern of our improved 3D gadget is constructed as follows, where all procedures are done for both $\sigma = L, R$.

- (1) Draw a perpendicular to ℓ_σ through B_σ for both $\sigma = L, R$, letting C be the intersection point.
- (2) Let ζ_σ for $\sigma = L, R$ be the critical angles defined in Definition 3.2. Choose a point D on the circular arc $B_L B_R$ with center A so that $\phi_\sigma = \angle B_\sigma A D$ satisfies

$$\phi_L \in [\gamma - 2\zeta_R, 2\zeta_L] \cap (0, \gamma), \quad \text{or equivalently, } \phi_R \in [\gamma - 2\zeta_L, 2\zeta_R] \cap (0, \gamma).$$
- (3) Let E_σ be the circumcenter of $\triangle B_\sigma C D$. Also, let m_σ be a ray parallel to and going in the same direction as ℓ_σ , starting from E_σ . Thus m_σ is a perpendicular bisector to segment $B_\sigma C$ and $A E_\sigma$ bisects $\angle B_\sigma A C$.
- (4) Let F be the intersection point of segments CD and $E_L E_R$. (This step is not directly related to the construction, but used later in Section 4.)
- (5) Determine a point G_σ on segment $A E_\sigma$ such that $\angle A B_\sigma G_\sigma = \pi - \beta_\sigma$.
- (6) If $\delta_\sigma > 0$, then determine a point H_σ on segment $A E_\sigma$ such that $\angle E_\sigma B_\sigma H_\sigma = \delta_\sigma$.
- (7) The crease pattern is shown as the solid lines in Figure 3.8, and the assignment of mountain folds and valley folds is given in Table 3.9, where we have two ways of assigning mountain folds and valley folds if both $\delta_\sigma > 0$ and $\phi_\sigma/2 < \zeta_\sigma$ hold.

	common creases	$\phi_\sigma/2 < \zeta_\sigma$ and		$\phi_\sigma/2 = \zeta_\sigma$ and	
		$\delta_\sigma = 0$	$\delta_\sigma > 0$	$\delta_\sigma = 0$	$\delta_\sigma > 0$
mountain folds	$j_\sigma, \ell_\sigma,$	$B_\sigma G_\sigma, D E_\sigma$	$D H_\sigma$	$B_\sigma E_\sigma = B_\sigma G_\sigma$	$B_\sigma E_\sigma,$
	$A B_\sigma, A D$		$B_\sigma E_\sigma, \mid B_\sigma H_\sigma,$ $B_\sigma G_\sigma \mid E_\sigma H_\sigma$		$D G_\sigma = D H_\sigma$
valley folds	$k_\sigma, m_\sigma,$	$A E_\sigma, D G_\sigma$	$D G_\sigma$	$A E_\sigma,$	$A E_\sigma,$
	$E_L E_R$		$A E_\sigma, \mid A H_\sigma,$ $B_\sigma H_\sigma \mid B_\sigma G_\sigma$	$D E_\sigma = D G_\sigma$	$B_\sigma G_\sigma = B_\sigma H_\sigma$

TABLE 3.9. Assignment of mountain folds and valley folds to the new gadget

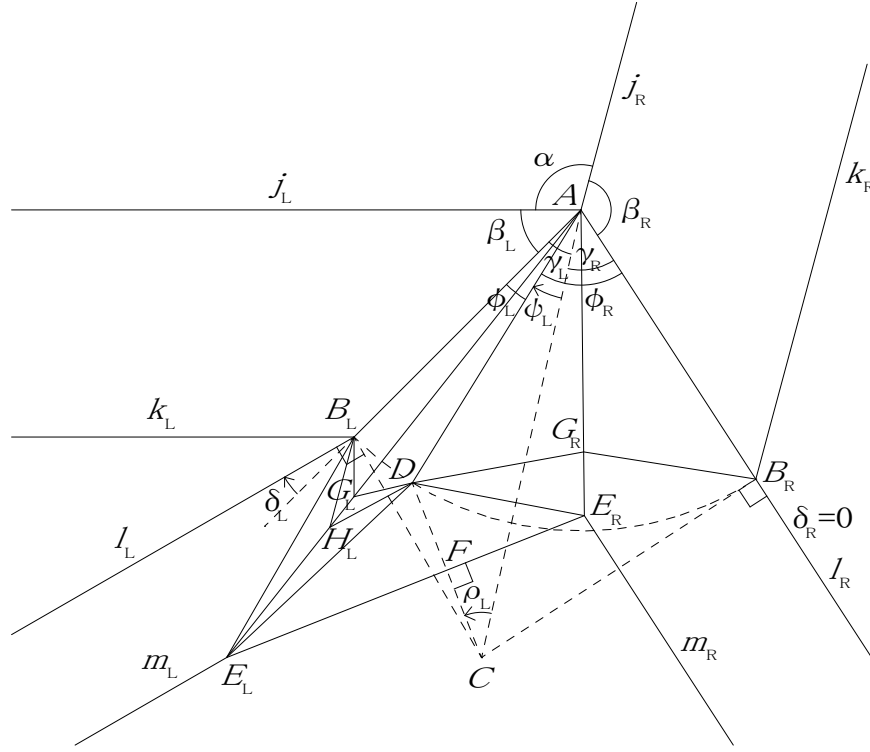


FIGURE 3.8. CP of our improved 3D gadget

The only difference between in the present and the previous ([1], Construction 3.2) constructions is the choice of point D on the circular arc $B_L B_R$ with center A . We show in Figure 3.10 the crease pattern of our improved 3D gadget for $\phi_L/2 = \zeta_L$. Also, we show in Figures 3.11 and 3.12 the crease patterns of our improved gadgets compatible with that constructed in Figure 2.3, where Figure 3.12 corresponds to the case $\phi_L/2 = \zeta_L$. Although there exists a compatible gadget for $\phi_R/2 = \zeta_R$, we omit the case because we need a large space to construct the crease pattern.

4. CONSTRUCTIBILITY AND FOLDABILITY OF THE CREASE PATTERN

In this section we discuss the validity of conditions (i)–(iv) given in Construction 3.7 to ensure that the construction is possible. Also, we check the foldability of the resulting crease pattern.

Conditions (i) and (ii) are the same as in Construction 2.2. To derive the necessity of condition (iii.a), we suppose the converse, i.e., $\delta_\sigma < 0$. Then $\angle k_\sigma B_\sigma \ell_\sigma = \pi - \beta_\sigma - \delta_\sigma$ is greater than $\angle \ell_\sigma B_\sigma G_\sigma = \pi - \beta_\sigma + \delta_\sigma$. Note that additional creases starting from B_σ can go only inside $\angle \ell_\sigma B_\sigma G_\sigma$ because creases going inside $\angle k_\sigma B_\sigma \ell_\sigma$ change angles between k_L and k_R and may produce other outgoing pleats. Thus the flat-foldability condition around B_σ , which is described as the vanishing of the alternative sum of $\angle k_\sigma B_\sigma \ell_\sigma$ and angles divided by the creases starting from B_σ and going inside $\angle \ell_\sigma B_\sigma G_\sigma$, can never hold. This is why we need condition (iii.a). Condition (iii.c) ensures that point C exists inside the angle formed by the extensions of ℓ_L and ℓ_R . Furthermore, for condition (iii.b), $\delta_\sigma < \beta_\sigma$ is necessary for Q_σ in Definition 3.2 to exist inside $\angle B_\sigma A B_{\sigma'}$. Also, $\delta_\sigma < \pi/2$ ensures that C exists inside $\angle B_L A B_R$, and thus $\gamma_\sigma = \angle B_\sigma A C$ calculated in [1], Lemma 4.1 as

$$\tan \gamma_\sigma = \frac{1 - \cos \gamma + \sin \gamma \tan \delta_{\sigma'}}{\sin \gamma + \cos \gamma \tan \delta_{\sigma'} + \tan \delta_{\sigma'}}$$

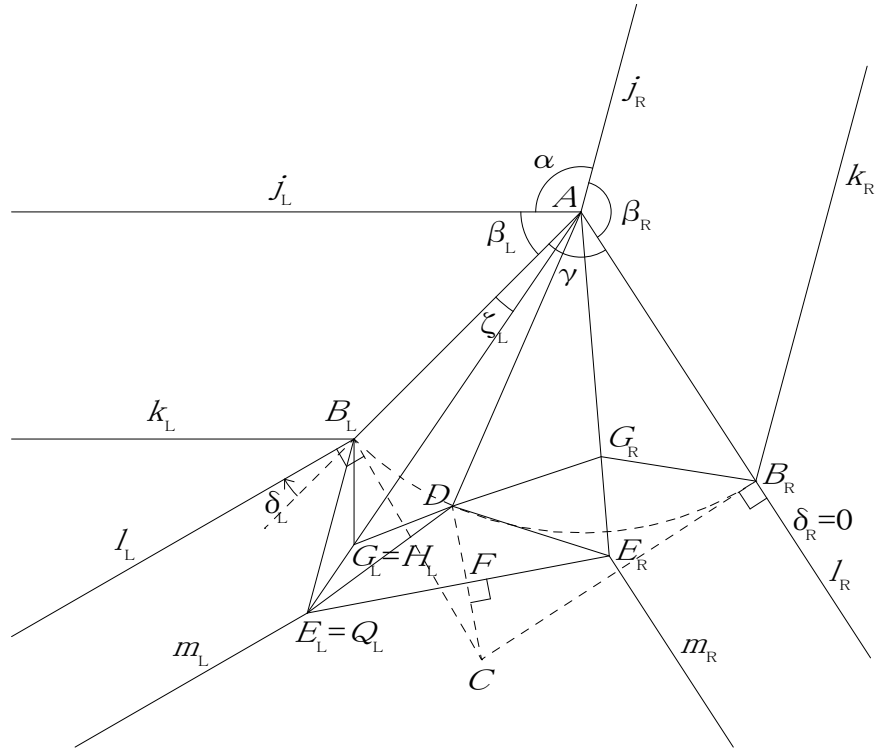


FIGURE 3.10. CP of our improved 3D gadget with $\phi_L/2 = \zeta_L$

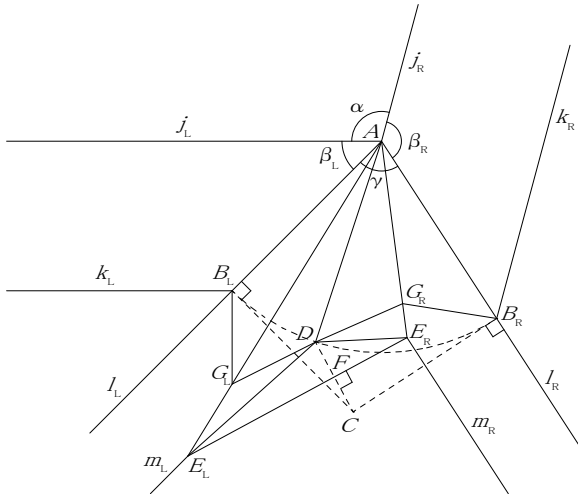


FIGURE 3.11. CP of our improved 3D gadget compatible with the conventional one shown in Figure 2.3

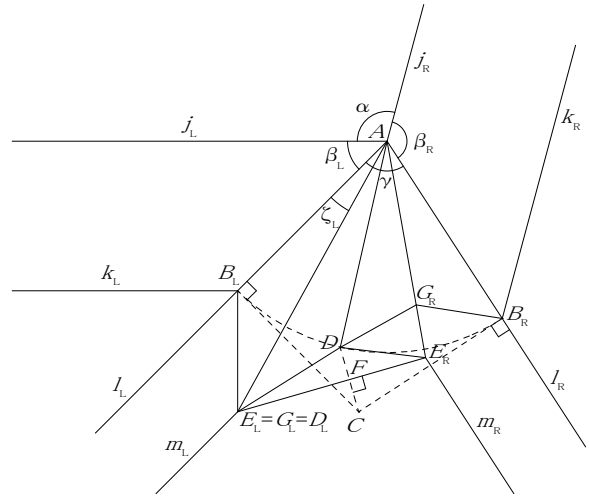


FIGURE 3.12. CP of our improved 3D gadget with $\phi_L/2 = \zeta_L$ compatible with the conventional one shown in Figure 2.3

is well-defined for $\sigma = L, R$. Note also that γ_σ has an alternative representation

$$\tan\left(\gamma_\sigma - \frac{\gamma}{2}\right) = \frac{\tan \delta_{\sigma'} - \tan \delta_\sigma}{2 + (\tan \delta_\sigma + \tan \delta_{\sigma'}) / \tan(\gamma/2)}.$$

The above conditions (i)–(iii) enable us to execute procedures (1)–(4) and construct points C , D and E_σ for $\sigma = L, R$. To deal with condition (iv), we consider when we can construct points G_σ and for $\delta_\sigma > 0$, H_σ in (5) and (6) of Construction 3.7. Note that in our construction, triangles $\triangle AB_L G_L$ and $\triangle AB_R G_R$ overlap on the left and the right face respectively, and thus in the crease pattern no crease is allowed to pass across these triangles. Thus the condition for constructing G_σ is that

$$(4.1) \quad \angle AB_\sigma G_\sigma \leq \angle AB_\sigma E_\sigma.$$

Also we see from procedure (6) that if G_σ exists and $\delta_\sigma > 0$, then the condition for constructing H_σ is written as

$$(4.2) \quad \angle AB_\sigma G_\sigma \leq \angle AB_\sigma H_\sigma.$$

Putting $\angle AB_\sigma G_\sigma = \pi - \beta_\sigma$ and $\angle AB_\sigma H_\sigma = \angle AB_\sigma E_\sigma - \delta_\sigma$ into (4.1) and (4.2), we therefore obtain the condition for constructing G_σ and H_σ that

$$(4.3) \quad \pi - \angle AB_\sigma E_\sigma \leq \beta_\sigma - \delta_\sigma,$$

which applies to both cases of $\delta_\sigma = 0$ and $\delta_\sigma > 0$. Furthermore, we can rewrite condition (4.3) in a more practical form as

$$(4.4) \quad \tan\left(\frac{\pi}{2} - \angle AB_\sigma E_\sigma\right) \leq \tan\left(\beta_\sigma - \delta_\sigma - \frac{\pi}{2}\right).$$

Theorem 4.1. *Suppose conditions (i)–(iii) of Construction 3.7 hold. Let D be a point on circular arc $B_L B_R$ with center A and let $\phi_\sigma = \angle B_\sigma A D$ for $\sigma = L, R$, so that $0 < \phi_\sigma < \gamma$ and $\phi_L + \phi_R = \gamma$. Then condition given by (4.3) that points G_σ and H_σ in Construction 3.7 are constructible is equivalent to*

$$(4.5) \quad \frac{\phi_\sigma}{2} \leq \zeta_\sigma,$$

where ζ_σ is given geometrically in Definition 3.2 or numerically in Proposition 3.6.

Proof. It suffices to prove the proposition assuming $\sigma = L$ and $A = (0, 0)$, $B_L = (1, 0)$. We see from $\angle B_L A P = \gamma/2$ and $\angle A B_L P = \gamma/2 + \delta_L + \delta_R$ that P is written as

$$(4.6) \quad P = p(1, c) = (1, 0) + q(1, -c')$$

for some $p, q \in \mathbb{R}$. Solving (4.6), we get

$$(p, q) = \frac{1}{c + c'}(c', c), \quad \text{so that } P = \frac{c'}{c + c'}(1, c).$$

Set $t_\sigma = \tan(\phi_\sigma/2)$. Since point E_L is the intersection point of the ray starting from A with slope t_L and the ray m_L starting from P with slope $-d_L$, E_L is written as

$$(4.7) \quad E_L = r(1, t_L) = \frac{c'}{c + c'}(1, c) + s(1, -d_L)$$

for some $r, s \in \mathbb{R}$. Solving (4.7), we get

$$(r, s) = \frac{c'}{(c + c')(t_L + d_L)}(-t_L + c, c + d_L), \quad E_L = \frac{c'(c + d_L)}{(c + c')(t_L + d_L)}(1, t_L).$$

This gives that

$$(4.8) \quad \begin{aligned} \overrightarrow{B_L E_L} &= E_L - (1, 0) \\ &= \frac{1}{(c + c')(t_L + d_L)}(c(c' - d_L) - (c + c')t_L, c'(c + d_L)t_L). \end{aligned}$$

Now putting (4.8) into condition (4.4) which is equivalent to (4.3), we have that

$$(4.9) \quad \begin{aligned} \tan\left(\frac{\pi}{2} - \angle AB_L E_L\right) &= \frac{(c + c')t_L - c(c' - d_L)}{c'(c + d_L)t_L} \\ &\leq -\frac{1}{b_L} = \tan\left(\beta_L - \delta_L - \frac{\pi}{2}\right). \end{aligned}$$

We have to be careful in dealing with this inequality because not c' and b_σ but their reciprocals are continuous functions with respect to β_σ, γ and δ_σ , while c, d_σ and t_σ are continuous themselves.

It follows from

$$-\frac{\pi}{2} < \frac{\gamma}{2} - \frac{\pi}{2} < \frac{\gamma}{2} + \delta_L + \delta_R - \frac{\pi}{2} < \frac{\pi}{2},$$

that

$$-\frac{1}{c} = \tan\left(\frac{\gamma}{2} - \frac{\pi}{2}\right) < \tan\left(\frac{\gamma}{2} + \delta_L + \delta_R - \frac{\pi}{2}\right) = -\frac{1}{c'},$$

and so we have $1/c' < 1/c$. Similarly, we have $1 - d_L/c', 1 + d_L/b_\sigma > 0$. Thus (4.9) is rewritten as

$$(4.10) \quad \frac{1/c + 1/c'}{1 + d_L/c} + \frac{1}{b_L} \leq \frac{1 - d_L/c'}{1 + d_L/c} \cdot \frac{1}{t_L}.$$

Consequently, using $1 + d_L/c, 1 - d_L/c' > 0$ and taking the arc tangents in (4.10) gives that

$$(4.11) \quad \tan^{-1}\left(\frac{1/c + 1/c' + (1 + d_L/c)/b_L}{1 - d_L/c'}\right) \leq \frac{\pi}{2} - \frac{\phi_L}{2}.$$

from which we obtain (4.5) for $\sigma = L$.

Note that the right-hand side of (4.10) is monotonically decreasing for $t_L \in (0, c]$, and also for $\phi_L \in (0, \gamma]$, and thus if (4.10) holds for $t = c$, then it holds for all $\phi_L \in (0, \gamma]$. Substituting $t = c$ into (4.10) gives $1/b_L \leq -1/c'$, which we can see is equivalent to

$$\frac{\pi}{2} - (\beta_L - \delta_L) \leq \frac{\gamma}{2} + \delta_L + \delta_R - \frac{\pi}{2}$$

by taking the arc tangents. Summing up, if $\beta_L + \gamma/2 + \delta_R \geq \pi$, then (4.10) holds for all $\phi_L \in (0, \gamma]$.

If $\beta_L + \gamma/2 + \delta_R \leq \pi$, then similarly as above we have $1/b_L + 1/c' \geq 0$. Thus together with $1 + d_L/b_L \geq 0$ and $1 - d_L/c' > 0$, we see that the argument of \tan^{-1} in (4.11) is positive. Hence in this case (4.11) is rewritten as

$$\frac{\phi_\sigma}{2} \leq \tan^{-1}\left(\frac{1 - d_L/c'}{1/c + 1/c' + (1 + d_L/c)/b_L}\right).$$

Therefore, we conclude that $\phi_L/2 \leq \zeta_L$, where ζ_L is given in Proposition 3.6. Also, interchanging subscripts L and R gives $\phi_R/2 \leq \zeta_R$. This completes the proof of Theorem 4.1. \square

Proposition 4.2. *Under condtions (i)–(iii) of Construction 3.7, if condtion (iv) holds then there exist points G_σ , and H_σ for $\delta_\sigma > 0$ in procedures (5) and (6).*

Proof. If condition (iv) of Construction 3.7 holds, then we can choose $\phi_\sigma \in (0, \gamma)$ so that $\phi_\sigma \leq 2\zeta_\sigma$ for both $\sigma = L, R$. Thus it follows from Theorem 4.1 that we can construct G_σ and H_σ . This completes the proof. \square

Theorem 4.3. *Define ψ_σ for $\sigma = L, R$ with $\psi_\sigma < \gamma_\sigma$ by*

$$\psi_\sigma = \angle B_\sigma AC - \angle B_\sigma AD = \gamma_\sigma - \phi_\sigma,$$

so that we have $\psi_L + \psi_R = 0$, $\phi_\sigma + \psi_\sigma = \gamma_\sigma$ and $-\gamma_{\sigma'} < \psi_\sigma < \gamma_\sigma$, where $\gamma_\sigma = \angle AB_\sigma C$. Also define ρ_σ for $\sigma = L, R$ by

$$\rho_\sigma = \angle ACE_\sigma - \angle DCE_\sigma.$$

Suppose conditions (i)–(iii) hold in Construction 3.7. Then our improved gadget is constructible if and only if we have for both $\sigma = L, R$ that

$$(4.12) \quad \beta_\sigma + \frac{\gamma_\sigma}{2} + \frac{\psi_\sigma}{2} + \rho_\sigma \geq \frac{\pi}{2}.$$

Furthermore, condition (4.12) is equivalent to

$$(4.13) \quad \beta_\sigma + \frac{\gamma_\sigma}{2} + \tan^{-1} \left(\frac{r+1}{r-1} \tan \frac{\psi_\sigma}{2} \right) \geq \frac{\pi}{2},$$

where $r > 0$ is the ratio of the length of segment AC to that of segment AB_σ given by

$$(4.14) \quad r = \frac{|AC|}{|AB|} = \frac{1}{\cos \gamma_\sigma - \sin \gamma_\sigma \tan \delta_\sigma}.$$

Before proving the theorem, we prove the following result, which will also be used in checking the foldability of the crease pattern.

Lemma 4.4. Define $\theta_\sigma, \eta_\sigma, \xi_\sigma$ and ρ_σ for $\sigma = L, R$ by

$$\theta_\sigma = \angle AB_\sigma E_\sigma - \angle AB_\sigma C, \quad \eta_\sigma = \angle AE_\sigma B_\sigma = \angle AE_\sigma D, \quad \xi_\sigma = \angle CE_\sigma F = \angle DE_\sigma F.$$

Then we have $\theta_\sigma + \eta_\sigma + \xi_\sigma = \pi/2$ and

$$(4.15) \quad \theta_\sigma = \frac{\gamma_\sigma}{2} + \frac{\psi_\sigma}{2} + \rho_\sigma, \quad \eta_\sigma = \frac{\pi}{2} - \gamma_\sigma - \delta_\sigma - \rho_\sigma, \quad \xi_\sigma = \frac{\gamma_\sigma}{2} + \delta_\sigma - \frac{\psi_\sigma}{2}.$$

Also, $\angle AB_\sigma E_\sigma$ is given by

$$(4.16) \quad \angle AB_\sigma E_\sigma = \frac{\pi}{2} + \frac{\gamma_\sigma}{2} + \delta_\sigma + \frac{\psi_\sigma}{2} + \rho_\sigma.$$

Proof. From the sum of the interior angles of $\triangle B_\sigma C E_\sigma$, we have

$$(4.17) \quad \theta_\sigma + \eta_\sigma + \xi_\sigma = \pi/2.$$

On the other hand, since $\angle AB_\sigma E$ can be written in two ways as

$$\begin{aligned} \angle AB_\sigma E_\sigma &= \angle AB_\sigma C + \theta_\sigma = \frac{\pi}{2} + \theta_\sigma + \delta_\sigma \\ &= \pi - \angle AE_\sigma B_\sigma - \angle B_\sigma A E_\sigma = \pi - \eta_\sigma - \frac{\gamma_\sigma - \psi_\sigma}{2}, \end{aligned}$$

from which it follows that

$$(4.18) \quad \theta_\sigma + \eta_\sigma = \frac{\pi}{2} - \frac{\gamma_\sigma - \psi_\sigma}{2} - \delta_\sigma,$$

Thus by (4.17) we have

$$\xi_\sigma = \frac{\gamma_\sigma - \psi_\sigma}{2} + \delta_\sigma.$$

It follows from the sum of the interior angles of $\triangle A C E_\sigma$ that

$$\begin{aligned} \pi &= \angle A E_\sigma C + \angle C A E_\sigma + \angle A C E_\sigma \\ &= (\eta_\sigma + 2\xi_\sigma) + \left(\gamma_\sigma - \frac{\gamma_\sigma - \psi_\sigma}{2} \right) + \left(\rho_\sigma + \frac{\pi}{2} - \xi_\sigma \right) \\ &= \pi - \theta_\sigma + \frac{\gamma_\sigma + \psi_\sigma}{2} + \rho_\sigma, \end{aligned}$$

where we used (4.17) in the last line, so that we have

$$(4.19) \quad \theta_\sigma = \frac{\gamma_\sigma + \psi_\sigma}{2} + \rho_\sigma.$$

Also, combining (4.18) and (4.19) and gives an expression for η_σ . This completes the proof of Lemma 4.4. \square

Proof of Theorem 4.3. Note that ρ_σ defined in Lemma 4.4 has the same sign as ψ_σ , and

$$(4.20) \quad \begin{aligned} \rho_L + \rho_R &= (\angle ACE_L - \angle DCE_L) + (\angle ACE_R - \angle DCE_R) \\ &= (\angle ACE_L + \angle ACE_R) - (\angle DCE_L + \angle DCE_R) = \angle E_L C E_R - \angle E_L C E_R = 0. \end{aligned}$$

We can calculate ρ_σ as

$$(4.21) \quad \rho_\sigma = \tan^{-1} \left(\frac{\sin \psi_\sigma}{r - \cos \psi_\sigma} \right),$$

where r is given by (4.14). Recall the condition that G_σ and H_σ in procedures (5) and (6) under conditions (i)–(iii) of Construction 3.7 is given by (4.3). Putting (4.16) into (4.3) gives the desired condition (4.12).

Now it remains to prove that (4.12) is equivalent to (4.13). Set $t_\sigma = \tan(\psi_\sigma/2)$. Then using $\sin \psi_\sigma = 2t_\sigma/(1+t_\sigma^2)$, $\cos \psi_\sigma = (1-t_\sigma^2)/(1+t_\sigma^2)$, we can express $\tan \rho_\sigma$ as

$$\tan \rho_\sigma = \frac{\sin \psi_\sigma}{r - \cos \psi_\sigma} = \frac{2t_\sigma}{(r+1)t_\sigma^2 + (r-1)}.$$

Also, by a straightforward calculation we have

$$\begin{aligned} t_\sigma + \tan \rho_\sigma &= \frac{(r+1)t_\sigma(1+t_\sigma^2)}{(r-1) + (r+1)t_\sigma^2}, \\ 1 - t_\sigma \tan \rho_\sigma &= \frac{(r-1)(1+t_\sigma^2)}{(r-1) + (r+1)t_\sigma^2}, \end{aligned}$$

from which it follows that

$$\tan \left(\frac{\psi_\sigma}{2} + \rho_\sigma \right) = \frac{t_\sigma + \tan \rho_\sigma}{1 - t_\sigma \tan \rho_\sigma} = \frac{r+1}{r-1} \tan \frac{\psi_\sigma}{2}.$$

Hence (4.12) is equivalent to (4.13), and the proof of Theorem 4.3 is complete. \square

Note that if point D lies on segment AC , then we have $\psi_L = \psi_R = \rho_L = \rho_R = 0$, so that (4.12) becomes

$$\beta_\sigma + \frac{\gamma_\sigma}{2} \geq \frac{\pi}{2},$$

which recovers [1], Construction 3.2, condition (iv).

Proposition 4.5. *In Construction 3.7, it is impossible for ζ_L and ζ_R in condition (iv) to satisfy $\zeta_L + \zeta_R = \gamma/2$. Equivalently, it is impossible for the equality in (4.12) to hold for both $\sigma = L, R$.*

Proof. Note that the equality $\phi_\sigma/2 = \zeta_\sigma$ in (4.5) and that in (4.12) are equivalent because both correspond to the equality in condition (4.3) by Theorems 4.1 and 4.3. Thus it is sufficient to prove that if equality in (4.12) holds for both $\sigma = L, R$ then $\alpha = \beta_L + \beta_R$, which results in a flat extrusion and does not satisfy condition (iv) of Construction 3.7.

Suppose equality in (4.12) holds for both $\sigma = L, R$, i.e.,

$$\beta_\sigma + \gamma_\sigma/2 + \psi_\sigma/2 + \rho_\sigma = \pi/2$$

holds for $\sigma = L, R$. Summing up the above equalities over $\sigma = L, R$ and using $\psi_L + \psi_R = \rho_L + \rho_R = 0$, we have $\beta_L + \beta_R + \gamma/2 = \pi = \alpha + \gamma/2$, from which it follows that $\alpha = \beta_L + \beta_R$ as desired. This completes the proof of Proposition 4.5. \square

Theorem 4.6. *The critical angles ζ_L and ζ_R defined in Definition 3.2 always satisfy $\zeta_L + \zeta_R > \gamma$. Therefore, condition (iv) of Construction 3.7 is unnecessary.*

We prepare the following two lemmas for proving Theorem 4.6.

Lemma 4.7. *We have $\beta_\sigma + \gamma_\sigma/2 > \pi/2$ for either or both of $\sigma = L, R$. Also, we have $\beta_L + \beta_R + \gamma/2 > \pi$.*

Proof. Suppose $\beta_\sigma + \gamma_\sigma/2 \leq \pi/2$ for both $\sigma = L, R$. Then we have $\beta_L + \beta_R + \gamma/2 \leq \pi$, which also implies $\alpha + \gamma/2 \geq \pi$. Thus we have $\beta_L + \beta_R \leq \alpha$, which contradicts condition (i) of Construction 3.7. This proves the first assertion. The second assertion follows immediately from $\beta_L + \beta_R + \gamma/2 > \alpha + \gamma/2$ and $\alpha + \beta_L + \beta_R + \gamma = 2\pi$. \square

Lemma 4.8. *We have*

$$(4.22) \quad \tan \frac{\gamma_\sigma}{2} = \frac{r-1}{r+1} \tan \left(\frac{\pi}{2} - \delta_\sigma \right).$$

Proof. If $\psi_\sigma = \gamma_\sigma$, then we have

$$(4.23) \quad \psi_\sigma/2 + \rho_\sigma|_{\psi_\sigma=\gamma_\sigma} = \pi - \angle AB_\sigma C = \pi/2 - \delta_\sigma.$$

On the other hand, we proved in the proof of Theorem 4.3 that

$$(4.24) \quad \tan \left(\frac{\psi_\sigma}{2} + \rho_\sigma \right) = \frac{r+1}{r-1} \tan \frac{\psi_\sigma}{2}.$$

Thus putting $\psi_\sigma = \gamma_\sigma$ in (4.24) and using (4.22), we obtain (4.22) as desired. \square

Proof of Theorem 4.6. By Lemma 4.7, $\beta_\sigma + \gamma_\sigma/2 > \pi/2$ holds for either or both of $\sigma = L, R$. If $\beta_\sigma + \gamma_\sigma/2 > \pi/2$ holds for both $\sigma = L, R$, then (4.13) holds for $\psi_L = \psi_R = 0$, which implies that $\phi_\sigma = \gamma_\sigma$ is certainly contained in $(\gamma - 2\zeta_\sigma, 2\zeta_\sigma)$. Thus condition (iv) holds. If not, we may suppose $\beta_L + \gamma_L/2 \leq \pi/2$ and $\beta_R + \gamma_R/2 > \pi/2$. Also, we have $\beta_R + \gamma_R/2 < \beta_R + \gamma/2 < \pi$.

Thus it remains to prove that condition (iv) holds if we have $\beta_L + \gamma_L/2 \leq \pi/2$ and $\pi/2 < \beta_R + \gamma_R/2 < \pi$. Now Choose ψ_L as

$$\frac{\psi_L}{2} = \tan^{-1} \left\{ \frac{r-1}{r+1} \tan \left(\frac{\pi}{2} - \beta_L - \frac{\gamma_L}{2} \right) \right\},$$

which is well-defined because we have $\pi/2 - \beta_L - \gamma_L/2 \in [0, \pi/2)$. Moreover, ψ_L is contained in $[0, \gamma_L)$ because we have that

$$\tan \frac{\psi_L}{2} = \frac{r-1}{r+1} \tan \left(\frac{\pi}{2} - \beta_L - \frac{\gamma_L}{2} \right) < \frac{r-1}{r+1} \tan \left(\frac{\pi}{2} - \delta_L \right) = \tan \frac{\gamma_L}{2},$$

where the inequality follows from

$$\left(\frac{\pi}{2} - \delta_L \right) - \left(\frac{\pi}{2} - \beta_L - \frac{\gamma_L}{2} \right) = (\beta_L - \delta_L) + \frac{\gamma_L}{2} > 0$$

by condition (iii.b) of Construction 3.7, and the last equality follows from Lemma 4.8. Then it suffices to prove that $\psi_R = -\psi_L$ satisfies (4.13) for $\sigma = R$ because then $\phi_L = \gamma_L - \psi_L$ is certainly contained in $(\gamma - 2\zeta_R, 2\zeta_L]$.

By the second assertion of Lemma 4.7, we have

$$(4.25) \quad \frac{\pi}{2} - \beta_L - \frac{\gamma_L}{2} < \beta_R + \frac{\gamma_R}{2} - \frac{\pi}{2}.$$

Since both sides of (4.25) are in the range $[0, \pi/2)$, we have that

$$\tan \left(\frac{\pi}{2} - \beta_L - \frac{\gamma_L}{2} \right) < \tan \left(\beta_R + \frac{\gamma_R}{2} - \frac{\pi}{2} \right) = -\tan \left(\frac{\pi}{2} - \beta_R - \frac{\gamma_R}{2} \right).$$

Thus we have

$$\tan \frac{\psi_R}{2} = -\tan \frac{\psi_L}{2} = -\frac{r-1}{r+1} \tan \left(\frac{\pi}{2} - \beta_L - \frac{\gamma_L}{2} \right) > \frac{r-1}{r+1} \tan \left(\frac{\pi}{2} - \beta_R - \frac{\gamma_R}{2} \right),$$

so that ψ_R satisfies (4.13) for $\sigma = R$ as desired. This completes the proof of Theorem 4.6. \square

There is also a more abstract proof of Theorem 4.6.

Alternative proof of Theorem 4.6. Fix α, β_σ and γ_σ for $\sigma = L, R$, and consider $\zeta = \zeta_L + \zeta_R - \gamma/2$ as a function of δ_L and δ_R . Suppose there exists a pair (a_L, a_R) of values of δ_L and δ_R satisfying conditions (i)–(iii) such that $(\delta_L, \delta_R) = (a_R, a_L)$ together with the given $(\alpha_\sigma, \beta_\sigma, \gamma_\sigma)$ for $\sigma = L, R$ satisfy condition (i)–(iii) of Construction 3.7 but does not satisfy condition (iv), i.e., $\zeta < 0$. Define a path $p(s) = (\delta_L(s), \delta_R(s)) = (s \cdot a_L, s \cdot a_R)$ and a function $\zeta(s) = \zeta_L(p(s)) + \zeta_R(p(s)) - \gamma/2$ for $s \in [0, 1]$. Then $p(s)$ satisfies condition (iii) for all $s \in [0, 1]$, and $\zeta(s)$ depends continuously on s . Also, we have $\zeta(0) > 0$ by Lemma 3.4 and $\zeta(1) < 0$. Thus by the intermediate value theorem, there exists $s_0 \in (0, 1)$ such that $\zeta(s_0) = 0$. However, then $(\alpha_\sigma, \beta_\sigma, \gamma_\sigma)$ do not satisfy condition (i) by Proposition 4.5, which is a contradiction. Hence $\zeta_L + \zeta_R > \gamma/2$ for all $(\alpha_\sigma, \beta_\sigma, \gamma_\sigma, \delta_\sigma)$ satisfying conditions (i)–(iii) of Construction 3.7. \square

We prove one more result which will be used in Section 6.

Proposition 4.9. *We have $\beta_\sigma + \gamma_\sigma/2 \leq \pi/2$ (resp. $\beta_\sigma + \gamma_\sigma/2 \geq \pi/2$) if and only if $\zeta_\sigma \leq \gamma_\sigma/2$ (resp. $\gamma_\sigma/2 \leq \zeta_\sigma$).*

Proof. First suppose $\zeta_\sigma \leq \gamma_\sigma/2$. Then we have that

$$\beta_\sigma + \frac{\gamma_\sigma}{2} = \beta_\sigma + \frac{\gamma_\sigma}{2} + \frac{\psi_\sigma}{2} + \rho_\sigma \Big|_{\psi_\sigma=0} \leq \beta_\sigma + \frac{\gamma_\sigma}{2} + \frac{\psi_\sigma}{2} + \rho_\sigma \Big|_{\psi_\sigma=\gamma_\sigma-2\zeta_\sigma} = \frac{\pi}{2}.$$

Next suppose $\beta_\sigma + \gamma_\sigma/2 \leq \pi/2$. Then since $\beta_\sigma + \gamma_\sigma/2 + \psi_\sigma/2 + \rho_\sigma = \pi/2$ holds for ψ_σ corresponding to ϕ_σ with $\phi_\sigma/2 = \zeta_\sigma$, we have that

$$\frac{\psi_\sigma}{2} + \rho_\sigma \Big|_{\psi_\sigma=\gamma_\sigma-2\zeta_\sigma} \geq 0,$$

from which $\zeta_\sigma \leq \gamma_\sigma/2$ follows as desired.

The assertion in the parentheses is proved by taking the contraposition and including the equality. This completes the proof of Proposition 4.9. \square

Now we shall check the foldability of the crease pattern resulting in Construction 3.7. For this purpose, we divide the crease pattern into two parts by polygonal chain $k_L B_L G_L D G_R B_R k_R$. Then we can see easily that the upper part forms the top and the side faces with flat back sides, where $\triangle A B_\sigma G_\sigma$ and $\triangle A D G_\sigma$ overlap with the side face $j_\sigma A B_\sigma k_\sigma$ for $\sigma = L, R$. Thus it remains to check that the lower part is flat-foldable to form the base of the extrusion. We show in Table 4.10 the adjacent vertices of or the rays starting from each vertex in the lower part, and for vertex D , we take into account both contributions from $\sigma = L, R$. Since vertices E_σ, H_σ are interior points of the lower part, we can check the flat-foldability around them by Kawasaki's theorem [2] (Murata-Kawasaki's theorem may be more precise) that the crease pattern is (locally) flat-foldable if and only if the alternative sum of the angles around each vertex vanishes. Note that k_σ and $B_\sigma G_\sigma$ around boundary point B_σ , and $G_\sigma B_\sigma$ and $G_\sigma D$ around boundary point G_σ overlap with each other, so that around B_σ and G_σ , the alternative sums of the angles contained in the lower part must also vanish. For boundary point D , $D G_L$ and $D G_R$, which overlap with k_L and k_R respectively, form an angle α . Thus around D , the alternative sum of the angles contained in the lower part must be α if we take the angle which contains $E_L E_R$ as positive. In view of the above, the flat-foldability around each vertex in the lower part is checked as follows.

- *Flat-foldability around B_σ .* If $\delta_\sigma = 0$, then the alternative sum of the angles around B_σ in the lower part is calculated as

$$\angle k_\sigma B_\sigma \ell_\sigma - \angle \ell_\sigma B_\sigma G_\sigma = \beta_\sigma - \beta_\sigma = 0.$$

	$\delta_\sigma = 0$ and $\beta_\sigma + \gamma_\sigma/2 + \psi_\sigma/2 + \rho_\sigma$		$\delta_\sigma > 0$ and $\beta_\sigma + \gamma_\sigma/2 + \psi_\sigma/2 + \rho_\sigma$	
	$> \pi/2$	$= \pi/2$	$> \pi/2$	$= \pi/2$
B_σ	$k_\sigma, \ell_\sigma, G_\sigma$		$k_\sigma, \ell_\sigma, E_\sigma, H_\sigma, G_\sigma$	$k_\sigma, \ell_\sigma, E_\sigma, G_\sigma = H_\sigma$
D	E_σ, G_σ	$E_\sigma = G_\sigma$	G_σ, H_σ	$G_\sigma = H_\sigma$
E_σ	$m_\sigma, D, E_{\sigma'}, G_\sigma$	$m_\sigma, B_\sigma, D, E_{\sigma'}$	$m_\sigma, B_\sigma, E_{\sigma'}, H_\sigma$	$m_\sigma, B_\sigma, E_{\sigma'}, G_\sigma = H_\sigma$
G_σ	B_σ, D, E_σ		B_σ, D, H_σ	B_σ, D, E_σ
H_σ	—		$B_\sigma, D, E_\sigma, G_\sigma$	

TABLE 4.10. Adjacent vertices of, or rays starting from each vertex in the lower part

If $\delta_\sigma > 0$, then we have

$$\begin{aligned}
 \angle k_\sigma B_\sigma \ell_\sigma &= \beta_\sigma - \delta_\sigma, \\
 \angle \ell_\sigma B_\sigma E_\sigma &= \pi + \delta_\sigma - \angle AB_\sigma E_\sigma = \frac{\pi}{2} - \theta_\sigma, \\
 \angle E_\sigma B_\sigma H_\sigma &= \delta_\sigma, \\
 \angle H_\sigma B_\sigma G_\sigma &= \angle AB_\sigma E_\sigma - \angle AB_\sigma G_\sigma - \angle E_\sigma B_\sigma H_\sigma \\
 &= \left(\frac{\pi}{2} + \theta_\sigma + \delta_\sigma \right) - (\pi - \beta_\sigma) - \delta_\sigma = \beta_\sigma + \theta_\sigma - \frac{\pi}{2}.
 \end{aligned}
 \tag{4.26}$$

Thus the alternative sum is given by

$$\begin{cases}
 \angle k_\sigma B_\sigma \ell_\sigma - \angle \ell_\sigma B_\sigma E_\sigma + \angle E_\sigma B_\sigma H_\sigma - \angle H_\sigma B_\sigma G_\sigma = 0 & \text{if } \beta_\sigma + \frac{\gamma_\sigma}{2} + \frac{\psi_\sigma}{2} + \rho_\sigma > \frac{\pi}{2}, \\
 \angle k_\sigma B_\sigma \ell_\sigma - \angle \ell_\sigma B_\sigma E_\sigma + \angle E_\sigma B_\sigma H_\sigma = 0 & \text{if } \beta_\sigma + \frac{\gamma_\sigma}{2} + \frac{\psi_\sigma}{2} + \rho_\sigma = \frac{\pi}{2},
 \end{cases}$$

where we used $\angle H_\sigma B_\sigma G_\sigma = \beta_\sigma + \theta_\sigma - \pi/2 = 0$ for β_σ .

• *Flat-foldability around D.* We divide $\angle E_R D E_L$ as

$$\angle E_R D E_L = \angle F D E_L + \angle F D E_R,$$

and consider the contributions to the alternative sum of angles around D from both sides separately.

If $\delta_\sigma = 0$, then we have

$$\begin{aligned}
 \angle F D E_\sigma &= \frac{\pi}{2} - \xi_\sigma = \theta_\sigma + \eta_\sigma, \\
 \angle E_\sigma D G_\sigma &= \angle A D E_\sigma - \angle A D G_\sigma = \angle A B_\sigma E_\sigma - \angle A B_\sigma G_\sigma \\
 &= \frac{\pi}{2} + \theta_\sigma - (\pi - \beta_\sigma) = \beta_\sigma + \theta_\sigma - \frac{\pi}{2},
 \end{aligned}
 \tag{4.27}$$

and thus

$$\begin{cases}
 \angle F D E_\sigma - \angle E_\sigma D G_\sigma = \pi - \beta_\sigma - \gamma_\sigma - \rho_\sigma & \text{if } \beta_\sigma + \frac{\gamma_\sigma}{2} + \frac{\psi_\sigma}{2} + \rho_\sigma > \frac{\pi}{2}, \\
 \angle F D E_\sigma = \frac{\pi}{2} - \frac{\gamma_\sigma}{2} + \frac{\psi_\sigma}{2} = \pi - \beta_\sigma - \gamma_\sigma - \rho_\sigma & \text{if } \beta_\sigma + \frac{\gamma_\sigma}{2} + \frac{\psi_\sigma}{2} + \rho_\sigma = \frac{\pi}{2}.
 \end{cases}
 \tag{4.28}$$

If $\delta_\sigma > 0$, then we have

$$\begin{aligned}
 \angle FDH_\sigma &= \angle FDE_\sigma + \angle E_\sigma DH_\sigma \\
 &= \left(\frac{\pi}{2} - \xi_\sigma\right) + \delta_\sigma = \theta_\sigma + \eta_\sigma + \delta_\sigma, \\
 \angle H_\sigma DG_\sigma &= \angle H_\sigma B_\sigma G_\sigma = \angle AB_\sigma E_\sigma - \angle AB_\sigma G_\sigma - \angle E_\sigma B_\sigma H_\sigma \\
 &= \left(\frac{\pi}{2} + \theta_\sigma + \delta_\sigma\right) - (\pi - \beta_\sigma) - \delta_\sigma = \beta_\sigma + \theta_\sigma - \frac{\pi}{2},
 \end{aligned}
 \tag{4.29}$$

and thus

$$\begin{cases}
 \angle FDH_\sigma - \angle H_\sigma DG_\sigma \\
 = \frac{\pi}{2} - \beta_\sigma + \eta_\sigma + \delta_\sigma = \pi - \beta_\sigma - \gamma_\sigma - \rho_\sigma & \text{if } \beta_\sigma + \frac{\gamma_\sigma}{2} + \frac{\psi_\sigma}{2} + \rho_\sigma > \frac{\pi}{2}, \\
 \angle FDE_\sigma = \frac{\pi}{2} - \frac{\gamma_\sigma}{2} + \frac{\psi_\sigma}{2} = \pi - \beta_\sigma - \gamma_\sigma - \rho_\sigma & \text{if } \beta_\sigma + \frac{\gamma_\sigma}{2} + \frac{\psi_\sigma}{2} + \rho_\sigma = \frac{\pi}{2}.
 \end{cases}
 \tag{4.30}$$

Consequently, in all cases we can calculate the alternative sum as

$$(\pi - \beta_L - \gamma_L - \rho_L) + (\pi - \beta_R - \gamma_R - \rho_R) = (2\pi - \beta_L - \beta_R - \gamma) - (\rho_L + \rho_R) = \alpha,$$

which coincide with the angle formed by k_L and k_R as desired, where we used (4.20).

• *Flat-foldability around E_σ .* Suppose $\delta_\sigma = 0$. Then we have

$$\begin{aligned}
 \angle m_\sigma E_\sigma G_\sigma &= \angle m_\sigma E_\sigma B_\sigma + \angle B_\sigma E_\sigma G_\sigma \\
 \angle m_\sigma E_\sigma F &= \angle m_\sigma E_\sigma C + \angle CE_\sigma F = \angle m_\sigma E_\sigma B_\sigma + \angle CE_\sigma F \\
 \angle FE_\sigma D &= \angle CE_\sigma F \\
 \angle DE_\sigma G_\sigma &= \angle B_\sigma E_\sigma G_\sigma,
 \end{aligned}$$

which gives that

$$\begin{cases}
 \angle m_\sigma E_\sigma G_\sigma - \angle m_\sigma E_\sigma F + \angle FE_\sigma D - \angle DE_\sigma G_\sigma = 0 & \text{if } \beta_\sigma + \frac{\gamma_\sigma}{2} + \frac{\psi_\sigma}{2} + \rho_\sigma > \frac{\pi}{2}, \\
 \angle m_\sigma E_\sigma B_\sigma - \angle m_\sigma E_\sigma F + \angle FE_\sigma D = 0 & \text{if } \beta_\sigma + \frac{\gamma_\sigma}{2} + \frac{\psi_\sigma}{2} + \rho_\sigma = \frac{\pi}{2}.
 \end{cases}$$

Next suppose $\delta_\sigma > 0$. Then we have

$$\begin{aligned}
 \angle m_\sigma E_\sigma F &= \angle m_\sigma E_\sigma C + \angle CE_\sigma F = \angle B_\sigma E_\sigma m_\sigma + \angle DE_\sigma F, \\
 \angle FE_\sigma G_\sigma &= \angle DE_\sigma F + \angle G_\sigma E_\sigma D = \angle DE_\sigma F + \angle G_\sigma E_\sigma B_\sigma,
 \end{aligned}$$

which gives that

$$\begin{cases}
 \angle B_\sigma E_\sigma m_\sigma - \angle m_\sigma E_\sigma F + \angle FE_\sigma G_\sigma - \angle G_\sigma E_\sigma B_\sigma = 0 & \text{if } \beta_\sigma + \frac{\gamma_\sigma}{2} + \frac{\psi_\sigma}{2} + \rho_\sigma > \frac{\pi}{2}, \\
 \angle B_\sigma E_\sigma m_\sigma - \angle m_\sigma E_\sigma F + \angle FE_\sigma G_\sigma = 0 & \text{if } \beta_\sigma + \frac{\gamma_\sigma}{2} + \frac{\psi_\sigma}{2} + \rho_\sigma = \frac{\pi}{2}.
 \end{cases}$$

• *Flat-foldability around G_σ and H_σ .* This is clear from the symmetry of B_σ and D with respect to AE_σ .

5. INTERFERENCE COEFFICIENTS AND THE DOWNWARD COMPATIBILITY THEOREM

Let us recall the definitions of interference coefficients introduced in [1], Section 5.

Definition 5.1. For a conventional 3D gadget in Construction 2.2, we define an *interference coefficient* $\kappa_{\text{conv}}(B_\sigma)$ of the conventional kind to be the ratio

$$\frac{|B_\sigma D_\sigma|}{h} = \frac{|B_\sigma D_\sigma|}{\lambda |AB|}$$

of the length of segment $B_\sigma D_\sigma$ to the height h of the extrusion, where $h = \lambda |AB|$ with λ given by

$$\lambda(\alpha, \beta_L, \beta_R) = \left(1 - \frac{\cos^2 \beta_L + \cos^2 \beta_R - 2 \cos \alpha \cos \beta_L \cos \beta_R}{\sin^2 \alpha} \right)^{1/2}.$$

Also, for an improved 3D gadget in Construction 3.7 with $\delta_L, \delta_R \geq 0$, let I'_σ be the intersection point of ray k_σ and polygonal chain $m_L E_L E_R m_R$ in the resulting extrusion (so that $B_L = B_R = B$). Then we define an *interference coefficient* $\kappa_{\text{in}}(B_\sigma)$ of the inner pleat to be the ratio

$$\frac{|BI'_\sigma|}{h} = \frac{|BI'_\sigma|}{\lambda |AB|}.$$

Similarly, we define an *interference coefficient* $\kappa_{\text{out}}(B_\sigma)$ of the outer pleat to be the ratio

$$\frac{|B_\sigma G_\sigma|}{h} = \frac{|B_\sigma G_\sigma|}{\lambda |AB|}.$$

Proposition 5.2. Assume $|AB| = 1$. For $\delta_L = \delta_R = 0$, the interference coefficient $\kappa_{\text{conv}}(B_\sigma)$ of the conventional kind is given by

$$(5.1) \quad \lambda \cdot \kappa_{\text{conv}}(B_\sigma) = |B_\sigma D_\sigma| = \frac{\tan(\gamma/2)}{2 \sin \beta_\sigma}.$$

Also, the interference coefficient $\kappa_{\text{out}}(B_\sigma)$ of the outer pleat is given by

$$\lambda \cdot \kappa_{\text{out}}(B_\sigma) = |B_\sigma G_\sigma| = \frac{1}{\sin \beta_\sigma / \tan(\phi_\sigma/2) - \cos \beta_\sigma}.$$

Set $\chi_\sigma = \beta_\sigma + \gamma_\sigma/2 + \psi_\sigma/2 + \rho_\sigma - \pi/2 - \delta_\sigma$. Then the interference coefficient $\kappa_{\text{in}}(B_\sigma)$ of the inner pleat is given by

$$(5.2) \quad 2\lambda \cdot \kappa_{\text{in}}(B_\sigma) = 2 |B_\sigma I'_\sigma| = \begin{cases} \frac{\cos \delta_{\sigma'} - \cos(\gamma + \delta_{\sigma'})}{\sin(\beta_\sigma - \delta_\sigma) \sin(\gamma + \delta_L + \delta_R)} & \text{if } \chi_\sigma \leq 0, \\ 2 |DI_\sigma| = \frac{\sqrt{r^2 - 2r \cos \psi_\sigma + 1}}{\cos(\pi - \beta_\sigma - \gamma_\sigma - \rho_\sigma)} \\ = -\frac{r^2 - 2r \cos \psi_\sigma + 1}{(r - \cos \psi_\sigma) \cos(\beta_\sigma + \gamma_\sigma) - \sin \psi_\sigma \sin(\beta_\sigma + \gamma_\sigma)} \\ = -\frac{c^2 + 2 - 2 \cos \phi_\sigma - 2c \sin \phi_\sigma}{\cos \beta_\sigma (1 - \cos \phi_\sigma) + (\sin \beta_\sigma - c) \sin \phi_\sigma} & \text{if } \chi_\sigma \geq 0, \end{cases}$$

where r is given by (4.14), $c = \tan(\gamma/2)$, and I_σ is the intersection point of segment $E_L E_R$ and (possibly an extension of) a reflection of DG_σ across DE_σ .

Proof. The expressions of κ_{conv} and κ_{out} are the same as in [1].

To calculate $\kappa_{\text{in}}(B_\sigma)$, first observe that DG_σ overlaps with k_σ and moves onto its reflection across AE_σ for $\delta_\sigma = 0$ and AH_σ for $\delta_\sigma > 0$ respectively. Thus in the resulting extrusion $E_L E_R$ intersects k_σ for $\delta_\sigma > 0$ if and only if $\angle H_\sigma DE_\sigma \leq \angle H_\sigma DG_\sigma$, which is equivalent to

$$\chi_\sigma = \beta_\sigma + \frac{\gamma_\sigma}{2} + \frac{\psi_\sigma}{2} + \rho_\sigma - \frac{\pi}{2} - \delta_\sigma \geq 0.$$

by (4.29), (4.15) and (4.26). This statement is also true for $\delta_\sigma = 0$ in which case $\chi_\sigma \geq 0$ holds by Theorem 4.3 and segment $E_L E_R$ intersects k_σ .

Suppose $\chi_\sigma \geq 0$. Then I'_σ is an intersection point of k_σ and m_σ in the resulting extrusion. Since $\angle E_\sigma I'_\sigma B_\sigma = \beta_\sigma - \delta_\sigma$ and the distance between B_σ and $E_\sigma I'_\sigma$ is equal to that between ℓ_σ and m_σ , which is given by $|B_\sigma C|/2$, we obtain the expression of κ_{in} for $\chi_\sigma \leq 0$.

Suppose $\chi_\sigma \geq 0$. Then $E_L E_R$ intersects k_σ at I_σ , and $\angle FDI_\sigma$ is calculated as

$$(5.3) \quad \angle FDI_\sigma = \begin{cases} \angle FE_\sigma D - \angle E_\sigma D G_\sigma = \pi - \beta_\sigma - \gamma_\sigma - \rho_\sigma & \text{if } \delta_\sigma = 0, \\ \angle FDH_\sigma - \angle H_\sigma D G_\sigma = \pi - \beta_\sigma - \gamma_\sigma - \rho_\sigma & \text{if } \delta_\sigma > 0 \end{cases}$$

by (4.28) and (4.30). Also, by the cosine theorem for $\triangle ACD$, we have

$$(5.4) \quad |CD| = \sqrt{r^2 - 2r \cos \psi_\sigma + 1}.$$

Hence (5.3) and (5.4) give the first expression of $\kappa_{\text{in}}(B_\sigma)$ for $\chi_\sigma \geq 0$. The second expression of $\kappa_{\text{in}}(B_\sigma)$ for $\chi_\sigma \geq 0$ is obtained by putting

$$\cos \rho_\sigma = \frac{r - \cos \psi_\sigma}{\sqrt{r^2 - 2r \cos \psi_\sigma + 1}}, \quad \sin \rho_\sigma = \frac{\sin \psi_\sigma}{\sqrt{r^2 - 2r \cos \psi_\sigma + 1}},$$

which are derived from (4.21), into

$$\cos(\pi - \beta_\sigma - \gamma_\sigma - \rho_\sigma) = -\cos(\beta_\sigma + \gamma_\sigma) \cos \rho_\sigma + \sin(\beta_\sigma + \gamma_\sigma) \sin \rho_\sigma$$

in the first expression of $\kappa_{\text{in}}(B_\sigma)$. Setting $c = \tan(\gamma/2)$ as in Proposition 3.6 and recalling $r = 1/\cos(\gamma/2)$ and $\psi_\sigma = \gamma/2 - \phi_\sigma$, we derive the last expression $\kappa_{\text{in}}(B_\sigma)$ by tedious but straightforward calculations. This completes the proof of Proposition 5.2. \square

Theorem 5.3 (Complete downward compatibility theorem). *Suppose $\delta_L = \delta_R = 0$. Then we have*

$$\kappa_{\text{in}}(B_\sigma) \leq \kappa_{\text{conv}}(B_\sigma), \quad \kappa_{\text{in}}(B_\sigma) \leq \kappa_{\text{conv}}(B_\sigma) \quad \text{for all } \phi_\sigma \in [\gamma - 2\zeta_\sigma, 2\zeta_\sigma] \cap (0, \gamma),$$

where both of the equalities hold if and only if $\phi_\sigma/2 = \zeta_\sigma$. Hence any conventional 3D gadget can always be replaced by any of our improved 3D gadgets compatible with it without affecting any other conventional 3D gadget.

Proof. For the first inequality, it suffices to prove $|B_\sigma D_\sigma| \geq |B_\sigma G_\sigma|$. Recalling that $\angle B_\sigma A D_\sigma = \zeta_\sigma$ and using (4.5), we have

$$\frac{1}{|B_\sigma D_\sigma|} = \frac{\sin \beta_\sigma}{\tan \zeta_\sigma} - \cos \beta_\sigma \leq \frac{\sin \beta_\sigma}{\tan(\phi_\sigma/2)} - \cos \beta_\sigma = \frac{1}{|B_\sigma G_\sigma|},$$

which gives $|B_\sigma D_\sigma| \geq |B_\sigma G_\sigma|$ as desired, where equality holds if and only if $\phi_\sigma/2 = \zeta_\sigma$.

For the second inequality, set $c = \tan(\gamma/2)$ as in Proposition 5.2. Then using (5.1) and the last expression of (5.2), we calculate as

$$\begin{aligned} 2|B_\sigma D_\sigma| - 2|DI_\sigma| &= \frac{c}{\sin \beta_\sigma} - \frac{c^2 + 2 - 2\cos \phi_\sigma - 2c \sin \phi_\sigma}{\{\cos \beta_\sigma(1 - \cos \phi_\sigma) + (\sin \beta_\sigma - c) \sin \phi_\sigma\}} \\ &= \frac{-(c \cos \beta_\sigma + 2 \sin \beta_\sigma)(1 - \cos \phi_\sigma) + c \sin \beta_\sigma \sin \phi_\sigma}{-\sin \beta_\sigma \{\cos \beta_\sigma(1 - \cos \phi_\sigma) + (\sin \beta_\sigma - c) \sin \phi_\sigma\}}. \end{aligned}$$

Since the denominator of the last term is positive, to prove $\kappa_{\text{in}}(B_\sigma) \leq \kappa_{\text{conv}}(B_\sigma)$, it suffices to prove that the numerator is nonnegative. Setting $t_\sigma = \tan(\phi_\sigma/2)$, we can express the numerator as

$$\begin{aligned} &-(c \cos \beta_\sigma + 2 \sin \beta_\sigma)(1 - \cos \phi_\sigma) + c \sin \beta_\sigma \sin \phi_\sigma \\ &= \frac{2t_\sigma}{1 + t_\sigma^2} \{c \sin \beta_\sigma - (c \cos \beta_\sigma + 2 \sin \beta_\sigma)t_\sigma\} \\ &= \frac{2t_\sigma(c \cos \beta_\sigma + 2 \sin \beta_\sigma)}{1 + t_\sigma^2} (\tan \zeta_\sigma - t_\sigma) \geq 0, \end{aligned}$$

where we used (3.7) and equality holds if and only if $\phi_\sigma/2 = \zeta_\sigma$. This proves $|B_\sigma D_\sigma| \geq |DI_\sigma|$, and therefore $\kappa_{\text{conv}}(B_\sigma) \geq \kappa_{\text{in}}(B_\sigma)$.

If we replace only one of two adjacent conventional 3D gadgets with our improved 3D gadget, then the interference of our gadget is κ_{in} or κ_{out} depending on whether its outgoing pleat is under or over the adjacent conventional gadget, while the interference of the conventional gadget remains

the same. Also, if we replace both of two adjacent conventional 3D gadgets with our improved 3D gadgets, then the sum of the interference of the resulting gadgets is the sum of κ_{in} of one gadget and κ_{out} of the other. Hence the sum of the interference in both cases always reduces after the replacement with our improved gadgets, which implies that the replacement is always possible. \square

6. EXAMPLES OF OUR IMPROVED 3D GADGETS

Given $\alpha_\sigma, \beta_\sigma, \gamma_\sigma$ and δ_σ for $\sigma = L, R$ satisfying condition (i)–(iii) of Construction 3.7, the range in circular arc $B_L B_R$ with center A in which D can move is determined by the critical angles ζ_L and ζ_R , and we can construct an improved gadget for each choice of the location of D , resulting the same appearance and outgoing pleats. Since it is troublesome to choose the location of D case by case, we naturally wonder what is the best choice. In this section we discuss some typical choices of ϕ_σ which are useful and satisfactory in some respects, not to say the best for all purposes.

Definition 6.1. In Construction 3.7, we say that our improved 3D gadget is *balanced* if $|\phi_L - \phi_R|$ is the smallest among all possible choices of ϕ_σ with fixed $\alpha_\sigma, \beta_\sigma, \gamma_\sigma$ and δ_σ . Also, we say that our 3D gadget is *left critical* (resp. *right critical*) if $\phi_L/2 = \zeta_L$ (resp. $\phi_R/2 = \zeta_R$), *critical* if it is either left or right critical, and *othogonal* if AC and $E_L E_R$ are orthogonal to each other. Our 3D gadget is orthogonal if and only if D lies on AC . Note that the 3D gadgets presented in our previous paper are classified as orthogonal gadgets in our terminology.

Suppose $\delta_L = \delta_R = 0$, so that $\gamma_\sigma = \gamma/2$. We may assume $\beta_L \leq \beta_R$ by interchanging L and R if necessary. Then from the proof of Lemma 4.7, $\beta_R + \gamma/4 > \pi/2$ always holds. Thus for a balanced 3D gadget we have that

$$\phi_L = \begin{cases} 2\zeta_L & \text{if } \beta_L + \frac{\gamma}{4} \leq \frac{\pi}{2}, \\ \frac{\gamma}{2} & \text{if } \beta_L + \frac{\gamma}{4} > \frac{\pi}{2}, \end{cases}$$

where the first equation follows because we have $\gamma - 2\zeta_R \leq 2\zeta_L \leq \gamma/2$ by Propositions 3.6 and 4.9. Therefore in this case a balanced 3D gadget is critical or orthogonal. Balanced 3D gadgets for $\delta_L = \delta_R = 0$ have the following features:

- The difference between ϕ_L and ϕ_R is minimized. (This is the origin of the name ‘balanced.’) This maximizes the apex angle $\phi_L/2$ of the left ear, i.e., the pleat formed by $\triangle B_L A G_L$ and $\triangle D A G_L$, which makes the resulting extrusion more stable.
- If $\beta_L + \gamma/4 \leq \pi/2$, then point E_L in the resulting crease pattern coincides with point D_L in Construction 2.2. Thus the crease pattern is easy to construct from that of the conventional one. Also, the crease pattern has least number of creases because points E_L and G_L are identical. These features make the crease pattern easier to fold.

In addition to the apex angles ϕ_σ of the ears of the gadget considered above, thin angles may also arise from $\angle E_\sigma D G_\sigma$ for $\delta_\sigma = 0$ and $\angle G_\sigma B_\sigma H_\sigma = \angle G_\sigma D H_\sigma$. If we define $\epsilon_\sigma \geq 0$ by

$$\epsilon_\sigma = \angle Q_\sigma B_\sigma E_\sigma = \angle A B_\sigma E_\sigma - \angle A B_\sigma Q_\sigma,$$

then we see from $\angle A B_\sigma Q_\sigma = \angle A B_\sigma G_\sigma + \delta_\sigma$ that

$$\epsilon_\sigma = \begin{cases} \angle E_\sigma D G_\sigma & \text{if } \delta_\sigma = 0, \\ \angle G_\sigma D H_\sigma & \text{if } \delta_\sigma > 0, \end{cases}$$

Also, ϵ_σ is written as

$$(6.1) \quad \epsilon_\sigma = \beta_\sigma + \gamma_\sigma/2 + \psi_\sigma/2 + \rho_\sigma - \pi/2$$

by (4.27), (4.29) and (4.19). Summing (6.1) over $\sigma = L, R$ gives

$$(6.2) \quad \epsilon_L + \epsilon_R = \beta_L + \beta_R + \gamma/2 - \pi.$$

Thus for $\delta_L = \delta_R = 0$ if $\beta_L + \gamma/4 - \pi/2$ is very small, then the balanced (and thus orthogonal) gadget has an unwelcome thin angle, and so it may be better to choose as $\phi_L/2 = \zeta_L$ so that the resulting gadget is left critical with $\epsilon_L = 0$ and $\epsilon_R = \beta_L + \beta_R + \gamma/2 - \pi$.

In general cases it is complicated to choose a value of ϕ_σ so that ϵ_σ has a desired value. However, we can control the values of ϵ_L and ϵ_R satisfying (6.2) by starting from finding the possible range of ϵ_σ instead of ϕ_σ , which gives an alternative construction of our improved 3D gadgets as follows.

Construction 6.2. Consider a development as in Figure 3.1 and require conditions (i)–(iii) of Construction 3.7. Then we can construct our improved 3D gadget as follows.

- (1) We begin with a resulting construction in Definition 3.2 as shown in Figure 3.3.
- (2) Choose and fix either of $\sigma = L$ or $\sigma = R$, and draw a ray u_σ starting from A and going inside $\angle B_\sigma A B_{\sigma'} = \gamma$ with $\angle B_\sigma A u_\sigma = \gamma/2 - \zeta_{\sigma'}$.
- (3) Let R_σ be the intersection point of u_σ and m_σ . Set $\bar{\epsilon}_\sigma$ as

$$\bar{\epsilon}_\sigma = \angle Q_\sigma B_\sigma R_\sigma = \begin{cases} \angle Q_\sigma B_\sigma R_\sigma & \text{if } \zeta_{\sigma'} < \gamma/2, \\ \pi - \angle A B_\sigma Q_\sigma = \beta_\sigma - \delta_\sigma & \text{if } \zeta_{\sigma'} = \gamma/2. \end{cases}$$

- (4) Set $\underline{\epsilon}_\sigma$ as

$$\underline{\epsilon}_\sigma = \begin{cases} 0 & \text{if } \zeta_\sigma < \gamma/2, \\ \angle Q_\sigma B_\sigma P = \beta_\sigma + \gamma/2 + \delta_{\sigma'} - \pi & \text{if } \zeta_\sigma = \gamma/2. \end{cases}$$

- (5) We can choose ϵ_σ as we like so that

$$(6.3) \quad \epsilon_\sigma \in \begin{cases} [\underline{\epsilon}_\sigma, \bar{\epsilon}_\sigma] \cap [0, \beta_\sigma - \delta_\sigma) & \text{if } \zeta_\sigma < \gamma/2, \\ (\underline{\epsilon}_\sigma, \bar{\epsilon}_\sigma] \cap [0, \beta_\sigma - \delta_\sigma) & \text{if } \zeta_\sigma = \gamma/2. \end{cases}$$

- (6) Draw a ray v_σ starting from B_σ and going outside $\angle A B_\sigma Q_\sigma$ with $\angle Q_\sigma B_\sigma v_\sigma = \epsilon_\sigma$, and let E_σ be the intersection point of v_σ and m_σ .
- (7) Set $\phi_\sigma = 2\angle B_\sigma A_\sigma E_\sigma$ and determine a point D on the circular arc $B_L B_R$ with center A such that $\angle B_\sigma A D = \phi_\sigma$.
- (8) Point $E_{\sigma'}$ on the other side of E_σ is determined as the intersection point of $m_{\sigma'}$ and the bisector of $\angle D A B_{\sigma'}$.
- (9) The construction up to here is shown in Figure 6.3. The rest of the construction is the same as procedures (5)–(7) of Construction 3.7.

Proposition 6.4. *In procedure (3) of Construction 6.2, we have $\angle Q_\sigma B_\sigma R_\sigma = \beta_L + \beta_R + \gamma/2 - \pi$ if $\zeta_{\sigma'} < \gamma/2$. Thus we can skip procedure (2) if we directly specify a value of ϵ_σ in procedure (5).*

Proof. If $\zeta_{\sigma'} < \gamma/2$, then the σ' -critical gadget exists, for which $\epsilon_{\sigma'} = 0$ holds and E_σ coincides with R_σ . Thus $\epsilon_\sigma = \angle Q_\sigma B_\sigma R_\sigma = \beta_L + \beta_R + \gamma/2 - \pi$ by (6.2). \square

With the following construction, we can avoid thin angles in the crease pattern arising from $\angle E_\sigma D G_\sigma$ or $\angle G_\sigma D H_\sigma$.

Example 6.5. We show in Figure 6.7 a crease pattern of an extruded pyramid of an isosceles right triangle standing on the largest rectangular face, in which there are four different 3D gadgets compatible with each other up to an inversion. The upper left, upper right, and lower left gadgets are critical, orthogonal, and balanced respectively, and the lower right is designed with Construction 6.2 so that $\epsilon_L = \epsilon_R$. We see that there arise thin angles in the lower left balanced gadget, and the upper left critical gadget is better for folding.

Example 6.6. The interference coefficients of the left critical cube gadget of height 1 are calculated from Proposition 5.2 as

$$\kappa_{\text{in,L}} = 1/4, \quad \kappa_{\text{out,L}} = 1/3, \quad \kappa_{\text{in,R}} = \kappa_{\text{out,R}} = 1/2,$$

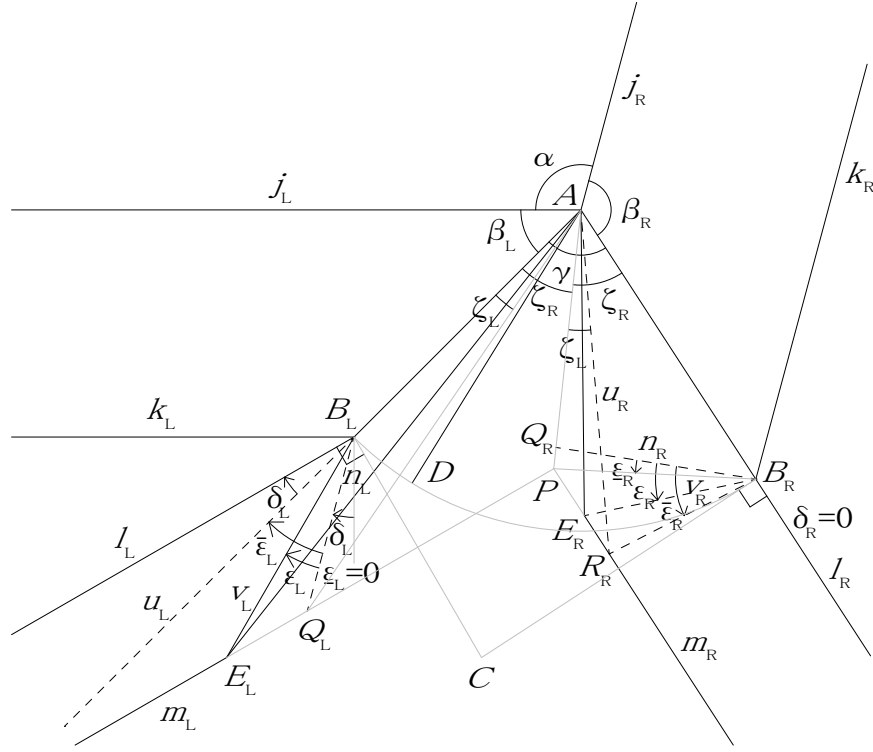


FIGURE 6.3. Alternative construction of our new gadget specifying ϵ_L or ϵ_R

where we denote $\kappa_{\text{in}}(B_\sigma)$ and $\kappa_{\text{out}}(B_\sigma)$ simply by $\kappa_{\text{in},\sigma}$ and $\kappa_{\text{out},\sigma}$. Thus if we place the left and the right critical cube gadgets of height 1 alternately, we can extrude a prism of a rectangle of dimensions $7/12 \times 1 \times 1$, whose crease pattern is shown in Figure 6.8. On the other hand, if we use only the left or the right critical cube gadgets of height 1, then we can extrude a square prism of dimensions $1 \times 1 \times 4/3$. However, as we will see in Example 6.9, we can make the extruded prism with the same square base as high as $1.416 (> \sqrt{2})$ with other cube gadgets.

Example 6.9. For an integer $n \geq 3$, consider an improved 3D gadget with $\alpha = (1 - 2/n)\pi$, $\beta_L = \beta_R = \pi/2$, $\gamma = 2\pi/n$ and $\delta_L = \delta_R = 0$. We can use n copies of this gadget to construct a prism of a regular polygon with n sides, so that each left and right ear is an inner and an outer pleat respectively. Then setting $c = \tan(\gamma/2)$ and $t_L = \tan(\phi_L/2)$, we calculate the interference coefficients as

$$\kappa_{\text{in},L} = \frac{1}{2} \cdot \frac{(c^2 + 4)t_L^2 - 4c \cdot t_L + c^2}{c \cdot t_L^2 - 2t_L + c}, \quad \kappa_{\text{out},R} = \frac{c - t_L}{1 + c \cdot t_L}.$$

Also, we have $\tan \zeta_L = \tan \zeta_R = c/2$, so that condition (4.5), which is now written as

$$\tan\left(\frac{\gamma}{2} - \zeta_R\right) \leq \tan \frac{\phi_L}{2} \leq \tan \zeta_L,$$

gives the range of t_L as

$$(6.4) \quad \frac{c}{c^2 + 2} \leq t_L \leq \frac{c}{2},$$

where $t_L = t_{L,0}$ with

$$(6.5) \quad t_{L,0} = \frac{\sqrt{c^2 + 1} - 1}{c}$$

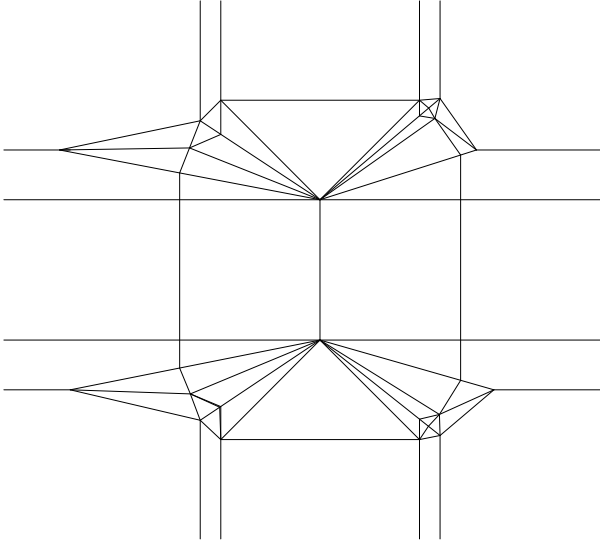


FIGURE 6.7. Four different 3D gadgets compatible with each other, used in a CP of an extruded pyramid standing on a rectangular face

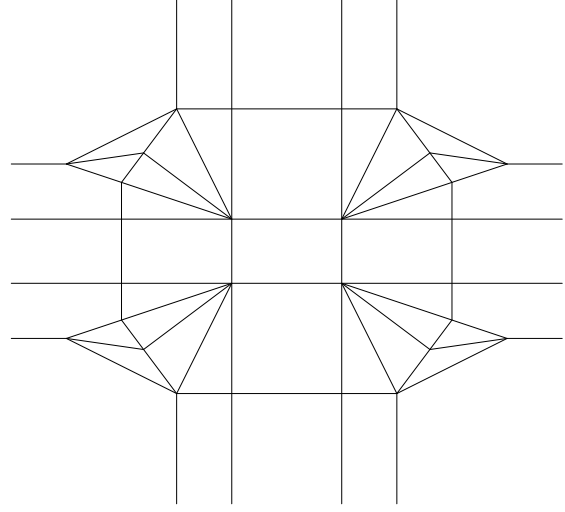


FIGURE 6.8. CP of a prism of a rectangle of dimensions $7/12 \times 1 \times 1$ extruded with the critical cube gadgets

corresponds to the orthogonal case $\phi_L = \psi_R = \gamma/2$, i.e., $\psi_L = \psi_R = 0$.

Now Let κ_{imp} be the sum of the above terms $\kappa_{\text{in,L}}$ and $\kappa_{\text{out,R}}$, considered as a function of t_L . Then all sides of the bottom face of the extruded prism have the same interference coefficient κ_{imp} . This κ_{imp} means the minimum side length of the regular n -gon in the bottom for the resulting prism of height 1. In other words, if the side length of the regular n -gon in the bottom is 1, then the maximum height of the resulting prism is given by κ_{imp}^{-1} . Define κ_{min} to be the minimum value of κ_{imp} for all t_L in the range (6.4). Also, define κ_0 to be the value of κ_{imp} for $t_{L,0}$ given by (6.5). We give in Table the minimum values κ_{min} , and the values of t_L, ϕ_L, ψ_L which attain κ_{min} for $n = 3, 4, 5, 6, 8, 12$, calculated to four significant figures. We also give the values of κ_{imp} for $\psi_L = 0$ and κ_{conv} for comparison.

Note that the 3D gadget which gives κ_{min} for $n = 4$ is almost orthogonal ($\kappa_{\text{imp}} = \kappa_0 = \sqrt{2}$ for the orthogonal gadget), that for $n = 6$ is almost critical ($\kappa_{\text{imp}} = 0.404145$ for the critical gadget, and $\kappa_{\text{min}} = 0.404133$ to six significant figures), and those for $n = 8$ and $n = 12$ are exactly critical.

7. DIVISION OF THE IMPROVED 3D GADGETS

In both of Constructions 2.2 and 3.7, since the paper is flat outside the extruded object, we can repeat the same gadgets to make the extrusion higher as long as no interference occurs. Changing the viewpoint, we can divide a gadget into smaller ones which extrude the same height in total. Although naive repetition of our 3D gadgets does not keep the back sides flat, we presented in [1], Section 8 a modification of our 3D gadgets for repetition with flat back sides, which we shall call *repeating gadgets*. Furthermore, we saw that these gadgets have no interference with other gadgets. In this section we present repeating gadgets which can be applied to our improved 3D gadgets. We shall deal with proportional division of a gadget into d gadgets in the ratio $p_1 : \dots : p_d$ with $p_1 + \dots + p_d = d$. Through this section, we will suppose $\delta_L = \delta_R = 0$.

Construction 7.1. Consider a development as shown in Figure 7.2, for which we require the following conditions.

n	3	4	5	6	8	12
κ_{\min}	1.133	0.7061	0.5153	0.4041	0.2836	0.1807
t_L attaining κ_{\min}	0.6670	0.4046	0.3044	0.2481	0.1907	0.1293
ψ_L ($^\circ$) attaining κ_{\min}	-7.404	0.9397	2.136	2.137	0.9018	0.2615
κ_0	1.155	0.7071	0.5257	0.4226	0.3066	0.1998
κ_{conv}	1.732	1	0.7265	0.5774	0.4142	0.2679
κ_{\min}^{-1}	0.8826	1.416	1.941	2.474	3.526	5.533
κ_0^{-1}	0.8660	1.414	1.902	2.366	3.262	5.005
$\kappa_{\text{conv}}^{-1}$	0.5774	1	1.376	1.732	2.414	3.732
$\kappa_{\min}^{-1}/\kappa_0^{-1}$	1.019	1.001	1.020	1.046	1.081	1.106
$\kappa_{\min}^{-1}/\kappa_{\text{conv}}^{-1}$	1.529	1.416	1.410	1.428	1.460	1.483

TABLE 6.10. Values of interference coefficients for the extrusion of the prism of a regular n -gon for various n , calculated to four significant figures

- (i) $\alpha < \beta_L + \beta_R$, $\beta_L < \alpha + \beta_R$ and $\beta_R < \alpha + \beta_L$.
- (ii) $\alpha + \beta_L + \beta_R < 2\pi$.
- (iii) $\alpha + \beta_L + \beta_R > \pi$.

Let ζ_L, ζ_R be the critical angles in Definition 3.2 and $\phi_L, \phi_R \in (0, \gamma)$ with $\phi_L + \phi_R = \gamma$ be chosen so that $\phi_\sigma \in [\gamma - 2\zeta_\sigma, 2\zeta_\sigma] \cap (0, \gamma)$. Then the crease pattern of the proportional division of our new 3D gadget into d gadgets in the ratio $p_1 : \dots : p_d$ from the bottom with $p_1 + \dots + p_d = d$ is constructed as follows, where all procedures are done for both $\sigma = L, R$, and the numbering of procedures corresponds to that in [1], Construction 8.1.

- (1) Draw a perpendicular to ℓ_σ through B_σ for both $\sigma = L, R$, letting C be the intersection point.
- (2) Divide segment CA (not AC) into d parts proportionally in the ratio $p_1 : \dots : p_d$, letting $A^{(1)}, \dots, A^{(d-1)}$ to be the divided points in order from the side of C .
- (3) For $n = 1, \dots, d-1$, draw a ray $\ell_\sigma^{(n)}$ parallel to ℓ_σ , starting from $A^{(n)}$ and going in the same direction as ℓ_σ , letting $B_\sigma^{(n)}$ be the intersection point with $B_\sigma C$.
- (4) For $n = 1, \dots, d$, let $E_\sigma^{(n)}$ be the intersection point of a bisector of $\angle B_\sigma^{(n)} A_\sigma^{(n)} C$ and a perpendicular bisector of $B_\sigma^{(n-1)} B_\sigma^{(n)}$, where we set $A^{(n)} = A, A^{(0)} = B_\sigma^{(0)} = C$ and $B_\sigma^{(n)} = B_\sigma$. Also, draw a ray $m_\sigma^{(n)}$ parallel to ℓ_σ , starting from $E_\sigma^{(n)}$ and going in the same direction as ℓ_σ . Thus we have $2d$ parallel rays $m_\sigma^{(1)}, \ell_\sigma^{(1)}, \dots, m_\sigma^{(n)}, \ell_\sigma^{(n)} = \ell_\sigma$ in order from the side of C .
- (5) For $n = 1, \dots, d$, let $F'^{(n)}$ be a point on segment $E_L E_R$ with $\angle E_L^{(n)} A^{(n)} F'^{(n)} = \phi_L^{(n)}$ (and so $\angle E_R^{(n)} A^{(n)} F'^{(n)} = \phi_R^{(n)}$). Here $\phi_L^{(n)}$ and $\phi_R^{(n)}$ satisfy $\phi_L^{(n)} + \phi_R^{(n)} = \gamma$ and

$$(7.1) \quad \tan \frac{\phi_\sigma^{(n)}}{2} \geq \frac{1}{1/\tan(\phi_\sigma^{(n-1)}/2) + 2/\tan(\gamma/2)}$$

for $n = 2, \dots, d$, where we set $\phi_\sigma^{(1)} = \phi_\sigma$.

Note that we can always choose $\phi_\sigma^{(n)}$ as $\phi_\sigma^{(n)} = \phi_\sigma^{(n-1)}$ because then (7.1) certainly holds. Thus we usually set $\phi_\sigma^{(2)} = \dots = \phi_\sigma^{(n)}$, which may differ from $\phi_\sigma^{(1)} = \phi_\sigma$. The meaning

of inequality (7.1) and a practical choice of $\phi_\sigma^{(n)}$ are explained in Remarks 7.6 and 7.9 respectively.

- (6) For $n = 1, \dots, d-1$, draw a ray $k_\sigma^{(n)}$ parallel to k_σ from $B_\sigma^{(n)}$ to the side of $m_\sigma^{(n+1)}$. If $k_\sigma^{(n)}$ intersects segment $A^{(n)}E_\sigma^{(n+1)}$, then let $G_\sigma^{(n)}$ be the intersection point. If not, then let $J_\sigma^{(n+1)}$ be the intersection point with $m_\sigma^{(n)}$.
- (7) For $n = 1, \dots, d$, draw a ray $k'_\sigma^{(n)}$ starting from $B_\sigma^{(n)}$ which is a reflection of $k_\sigma^{(n)}$ across $\ell_\sigma^{(n)}$, where we set $k_\sigma^{(d)} = k_\sigma$. If $k'_\sigma^{(n)}$ intersects segment $A^{(n)}E_\sigma^{(n)}$, then let $G_\sigma^{(n)}$ be the intersection point. If not, then it $k'_\sigma^{(n)}$ intersects $m_\sigma^{(n)}$ at $J_\sigma^{(n)}$ given in (6). Note that $G_\sigma^{(1)}$ always exists, and for $2 \leq n \leq d$, $G_\sigma^{(n)}$ exists if and only if $G_\sigma^{(n-1)}$ exists.
- (8) For $n = 1, \dots, d$, draw a circle with center $A^{(n)}$ through $B_L^{(n)}$ and $B_R^{(n)}$. If the circle intersects segment $A^{(n)}F'^{(n)}$ excluding endpoint $F'^{(n)}$, then let $D^{(n)}$ be the intersection point, and if $n \leq d-1$ and it intersects segment $A^{(n)}F'^{(n+1)}$ excluding endpoint $F'^{(n+1)}$, then let $D'^{(n)}$ be the intersection point. Note that $D^{(1)} = D$ always exists. Also, as we will see in (7.2) in Lemma 7.5, we have

$$\left| A^{(n)}F'^{(n)} \right| - \left| A^{(n)}B_\sigma^{(n)} \right| = \left| A^{(n-1)}F'^{(n)} \right| - \left| A^{(n-1)}B_\sigma^{(n-1)} \right| \quad \text{for } 2 \leq n \leq d,$$

which implies that $D^{(n)}$ exists if and only if $D'^{(n-1)}$ exists.

- (9) For $n = 2, \dots, d$ such that $D^{(n)}$ and $D'^{(n-1)}$ in (8) exist, draw a parallel line to segment $D^{(1)}E_\sigma^{(1)}$ through $D^{(n)}$ and a parallel line to segment $D^{(1)}E_\sigma^{(1)}$ through $D'^{(n-1)}$, letting $K_\sigma^{(n)}$ be the common intersection point with segment $E_L^{(n)}E_R^{(n)}$.
- (10) For $n = 2, \dots, d$ such that $D^{(n)}$ and $D'^{(n-1)}$ in (8) exist, draw a ray starting from $D^{(n)}$ which is a reflection of $k'_\sigma^{(n)}$ across $A^{(n)}E_\sigma^{(n)}$. If the ray intersects $A^{(n)}E_\sigma^{(n)}$, then $G_\sigma^{(n)}$ is the intersection point. If not, then the ray intersects $E_L^{(n)}E_R^{(n)}$, letting $M_\sigma^{(n)}$ be the intersection point. Also, draw a ray starting from $D'^{(n-1)}$ which is a reflection of $k_\sigma^{(n-1)}$ across $A^{(n-1)}E_\sigma^{(n)}$. Then the ray passes through $G_\sigma^{(n-1)}$ (resp. $M_\sigma^{(n)}$) if $G_\sigma^{(n-1)}$ exists (resp. does not exist).
- (11) For $n = 2, \dots, d$ such that $G_\sigma^{(n)}, G_\sigma^{(n-1)}$ exist and $D^{(n)}, D'^{(n-1)}$ do not, draw a line through $G_\sigma^{(n)}$ which is a reflection of $k'_\sigma^{(n)}$ across $A^{(n)}E_\sigma^{(n)}$, and a line through $G_\sigma^{(n-1)}$ which is a reflection of $k'_\sigma^{(n)}$ across $A^{(n)}E_\sigma^{(n)}$, letting $M_\sigma^{(n)}$ be their common intersection point with segment $E_L^{(n)}E_R^{(n)}$. (If the two lines overlap $E_L^{(n)}E_R^{(n)}$, which happens only if $\left| A^{(n)}F'^{(n)} \right| = \left| A^{(n)}B_\sigma^{(n)} \right|$ and $G_\sigma^{(n)} = G_\sigma^{(n-1)} = E_\sigma^{(n)}$, then let $M_\sigma^{(n)} = E_\sigma^{(n)}$.)
- (12) The crease pattern is shown as the solid lines in Figure 7.3, and the assignment of mountain folds and valley folds is given in Table 7.4 if $\phi_\sigma/2 < \zeta_\sigma$, and Table 7.12 if $\phi_\sigma/2 = \zeta_\sigma$.

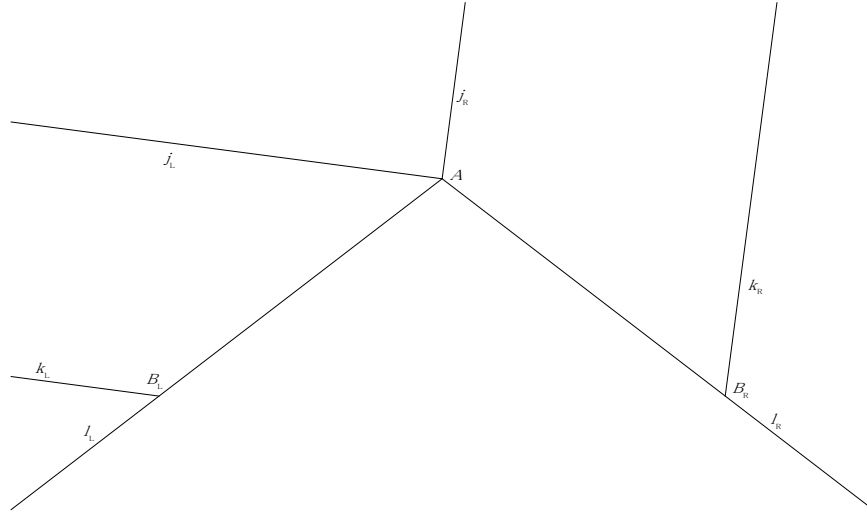
Lemma 7.5. Suppose $|AB| = d$ and let $q_n = p_1 + \dots + p_n$, so that $\left| A^{(n)}B_\sigma^{(n)} \right| = q_n$. Then we have

$$\left| A^{(n-1)}F'^{(n)} \right| = \left\{ \frac{r^2 - 1}{2(r \cos \psi_L - 1)} - 1 \right\} \cdot p_n, \quad \left| A^{(n)}F'^{(n)} \right| = \frac{r^2 - 1}{2(r \cos \psi_L - 1)} \cdot p_n.$$

Also, we have

$$(7.2) \quad \left| A^{(n-1)}F'^{(n)} \right| - \left| A^{(n-1)}B_\sigma^{(n-1)} \right| = \left| A^{(n)}F'^{(n)} \right| - \left| A^{(n)}B_\sigma^{(n)} \right|.$$

Proof. Let $F^{(n)}$ be the intersection point of segment AC and $E_L^{(n)}E_R^{(n)}$. Also, set $\psi_\sigma^{(n)} = \gamma/2 - \phi_\sigma^{(n)}$ and let $\rho_\sigma^{(n)}$ correspond to $\psi_\sigma^{(n)}$. Then we can see easily that $\angle A^{(n)}F^{(n)}F'^{(n)} = \pi/2 + \rho_\sigma^{(n)}$ and


 FIGURE 7.2. Development to which we apply d 3D gadgets successively

	common creases	n with $2 \leq n \leq d$ such that			
		$\exists D^{(n)} \exists G_\sigma^{(n)}$	$\exists D^{(n)} \nexists G_\sigma^{(n)}$	$\nexists D^{(n)} \exists G_\sigma^{(n)}$	$\nexists D^{(n)} \nexists G_\sigma^{(n)}$
mountain folds	$j_\sigma, \ell_\sigma^{(n)},$ $AB_\sigma, A^{(1)}D^{(1)},$ $B_\sigma^{(1)}G_\sigma^{(1)}, D^{(1)}E_\sigma^{(1)}$	$A^{(n-1)}E_\sigma^{(n)}$ $A^{(n)}D^{(n)}, D^{(n)}K_\sigma^{(n)}$		$(A^{(n-1)}E_L^{(n)}, A^{(n-1)}E_R^{(n)})^*,$ $A^{(n)}F'^{(n)}$	
		$B_\sigma^{(n-1)}G_\sigma'^{(n-1)},$ $D_\sigma'^{(n-1)}G_\sigma'^{(n-1)}$	$B_\sigma^{(n)}J_\sigma^{(n)},$ $D_\sigma'^{(n-1)}M_\sigma^{(n)}$	$B_\sigma^{(n-1)}G_\sigma'^{(n-1)},$ $G_\sigma'^{(n-1)}M_\sigma^{(n)}$	$B_\sigma^{(n)}J_\sigma^{(n)}$
valley folds	$k_\sigma, m_\sigma^{(n)},$ $A^{(n)}E_\sigma^{(n)}, E_L^{(n)}E_R^{(n)},$ $D^{(1)}G_\sigma^{(1)}$	$A^{(n-1)}D'^{(n-1)}, D'^{(n-1)}K_\sigma^{(n)}$		$A^{(n-1)}F'^{(n)}, (E_L^{(n)}E_R^{(n)})^*$	
		$B_\sigma^{(n-1)}G_\sigma^{(n)},$ $D^{(n)}G_\sigma^{(n)}$	$B_\sigma^{(n-1)}J_\sigma^{(n)},$ $D^{(n)}M_\sigma^{(n)}$	$B_\sigma^{(n-1)}G_\sigma^{(n)},$ $G_\sigma^{(n)}M_\sigma^{(n)}$	$B_\sigma^{(n-1)}J_\sigma^{(n)}$

 TABLE 7.4. Assignment of mountain folds and valley folds for the division of the new gadget, where the folds of starred creases can be inverted at the same time for individual $n \geq 2$

$\angle F^{(n)} A^{(n)} F'^{(n)} = \psi_L^{(n)}$. Thus $|A^{(n-1)} F'^{(n)}| + |A^{(n)} F'^{(n)}|$ is calculated as

$$\begin{aligned}
 (7.3) \quad |A^{(n-1)} F'^{(n)}| + |A^{(n)} F'^{(n)}| &= \frac{|A^{(n-1)} A^{(n)}|}{\cos \psi_L^{(n)} - \sin \psi_L^{(n)} \tan \rho_L^{(n)}} \\
 &= \frac{r |A^{(n)} B^{(n)}|}{\cos \psi_L^{(n)} - \sin^2 \psi_L^{(n)} / (r - \cos \psi_L^{(n)})} = \frac{r(r - \cos \psi_L^{(n)})}{r \cos \psi_L^{(n)} - 1} \cdot p_n,
 \end{aligned}$$

where we used (4.21) in the first equality in the second line. On the other hand, since $E_L^{(n)} E_R^{(n)}$ is a perpendicular bisector of $A^{(n-1)} A^{(n)}$, we have for $n = 1$

$$|A^{(1)} F'^{(1)}| = |A^{(1)} D^{(1)}| + |D^{(1)} F'^{(1)}| = p_1 + |A^{(0)} F'^{(1)}|,$$

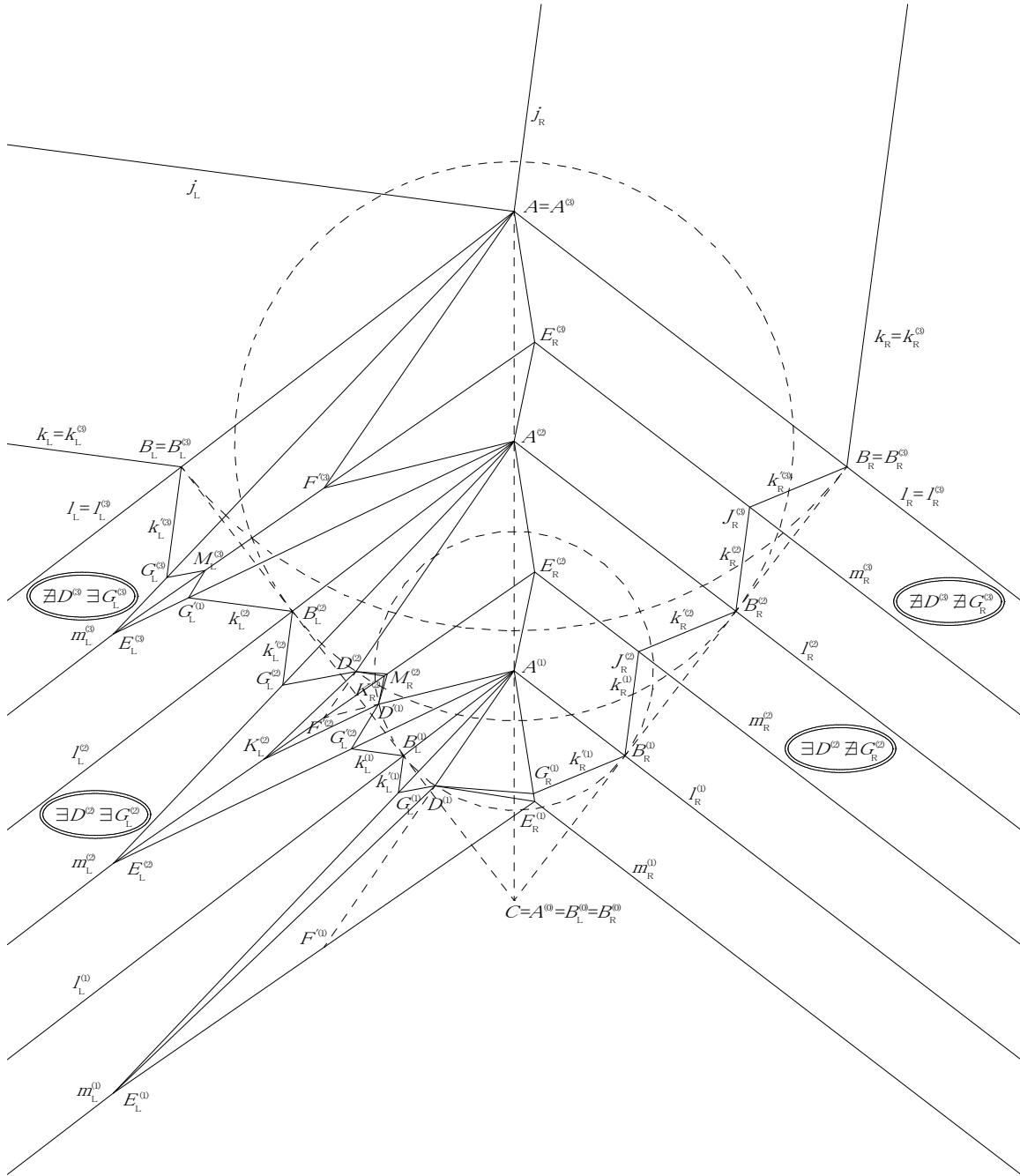


FIGURE 7.3. CP of the division of our improved 3D gadget

and similarly that for all n

$$(7.4) \quad \left| A^{(n)} F'^{(n)} \right| = \left| A^{(n)} D^{(n)} \right| + \left| D^{(n)} F'^{(n)} \right| = p_n + \left| A^{(n-1)} F'^{(n)} \right|.$$

Thus by (7.3) and (7.4), we have

$$\left| A^{(n-1)} F'^{(n)} \right| = \left\{ \frac{r^2 - 1}{2(r \cos \psi_L^{(n)} - 1)} - 1 \right\} \cdot p_n, \quad \left| A^{(n)} F'^{(n)} \right| = \frac{r^2 - 1}{2(r \cos \psi_L^{(n)} - 1)} \cdot p_n.$$

Consequently, we have

$$\begin{aligned} \left| A^{(n-1)} F'^{(n)} \right| - \left| A^{(n-1)} B_\sigma^{(n-1)} \right| &= \frac{r^2 - 1}{2(r \cos \psi_L^{(n)} - 1)} \cdot p_n - p_n - (p_1 + \cdots + p_{n-1}) \\ &= \frac{r^2 - 1}{2(r \cos \psi_L^{(n)} - 1)} \cdot p_n - q_n = \left| A^{(n)} F'^{(n)} \right| - \left| A^{(n)} B_\sigma^{(n)} \right|. \end{aligned}$$

This completes the proof. \square

Remark 7.6. Inequality (7.1) is equivalent to

$$\angle E_\sigma^{(n)} A^{(n-1)} \ell_\sigma^{(n-1)} \geq \angle E_\sigma^{(n-1)} A^{(n-1)} \ell_\sigma^{(n-1)} = \phi_\sigma^{(n-1)},$$

which is necessary when crease $A^{(n-1)} E_\sigma^{(n)}$ is a mountain fold, but unnecessary when $D^{(n)}$ does not exist and $A^{(n-1)} E_\sigma^{(n)}$ is inverted to a valley fold in Table 7.4.

In Construction 7.1, (8), if $D'^{(n)}$ exists, then $D'^{(n)}$ overlaps with $D^{(n)}$ because of $|A^{(n)} D^{(n)}| = |A^{(n)} D'^{(n)}| = p_1 + \cdots + p_n$. Also, if $D'^{(n)}$ exists, then $D^{(n+1)}$ overlaps with $D'^{(n)}$ by (7.2). Thus $D^{(n)}$ and $D'^{(n-1)}$ overlap with $D^{(1)}$ as long as they exist. In other words, if $D^{(n)}$ exists, then $\triangle A^{(n)} E_L^{(n)} E_R^{(n)}$ overlaps with the innermost point $D^{(1)}$ of the tongue of the lowest gadget. Also, if $D'^{(n-1)}$ exists, then $\triangle A^{(n-1)} E_L^{(n)} E_R^{(n)}$ overlaps with $D^{(1)}$.

Proposition 7.7. Suppose $n \geq 2$ and let $q_n = p_1 + \cdots + p_n$. Then points $D^{(n)}$ and $D'^{(n-1)}$ given in Construction 7.1, (8) exist if and only if

$$q_n < \frac{r^2 - 1}{2(r \cos \psi_L^{(n)} - 1)} \cdot p_n.$$

In particular, suppose $p_1 = \cdots = p_d = 1$ (equal division). Then if $D^{(n)}$ does not exist for some n , then neither do $D^{(m)}$ for all $m > n$ if we set $\psi_\sigma^{(m)} = \psi_\sigma^{(n)}$.

Proposition 7.8. Suppose $n \geq 2$ and let $q_n = p_1 + \cdots + p_n$ as before. In Construction 7.1, points $G_\sigma^{(n)}$ and $G_\sigma'^{(n-1)}$ given in (7) exist if and only if

$$q_n < \frac{\tan(\gamma/2)}{2} \left(\frac{1}{\tan(\phi_\sigma^{(n)}/2)} - \frac{1}{\tan \beta_\sigma} \right) \cdot p_n.$$

In particular, suppose $p_1 = \cdots = p_d = 1$ (equal division). Then if $G^{(n)}$ does not exist for some n , then neither do $G^{(m)}$ for all $m > n$ if we set $\psi_\sigma^{(m)} = \psi_\sigma^{(n)}$.

Remark 7.9. We chose as $\alpha = 90^\circ$, $\beta_L = 45^\circ$, $\beta_R = 120^\circ$, $\gamma = 105^\circ$, $\phi_L^{(n)} = 18^\circ$, $\psi_L^{(n)} = 34.5^\circ$ for all n and $p_1 = p_2 = p_3 = 1$ in Construction 7.1, so that all cases in Table 7.4 appear in Figure 7.3. Indeed, since we have

$$\frac{r^2 - 1}{2(\cos \psi_L^{(n)} - 1)} \approx 2.4004, \quad \frac{\tan(\gamma/2)}{2} \left(\frac{1}{\tan(\phi_\sigma^{(n)}/2)} - \frac{1}{\tan \beta_\sigma} \right) \approx \begin{cases} 3.4625 & \text{for } \sigma = L, \\ 1.0629 & \text{for } \sigma = R, \end{cases}$$

we see from Proposition 7.7 that $D^{(n)}$ exists only for $n = 2$, $G_R^{(n)}$ exists for $n = 2, 3$, while no $G_L^{(n)}$ exists.

The above choice of ϕ_L is instructive, but not practical. If we choose $\phi_L^{(n)} = 2\zeta_L \approx 43.062^\circ$ instead, which leads to

$$\frac{r^2 - 1}{2(\cos \psi_L^{(n)} - 1)} \approx 1.3687, \quad \frac{\tan(\gamma/2)}{2} \left(\frac{1}{\tan(\phi_\sigma^{(n)}/2)} - \frac{1}{\tan \beta_\sigma} \right) \approx \begin{cases} 0.99998 & \text{for } \sigma = L, \\ 1.4620 & \text{for } \sigma = R, \end{cases}$$

then the crease pattern becomes much simpler as in Figure 7.10 because the smaller $|\psi_L|$ is, the less number of $D^{(n)}$ exist. If we choose as $\phi_L^{(n)} = \phi_R^{(n)} = \gamma/2$ for $n = 2, 3$, we can also avoid the appearance of $D^{(n)}$ and $G^{(n)}$ for $n = 2, 3$.

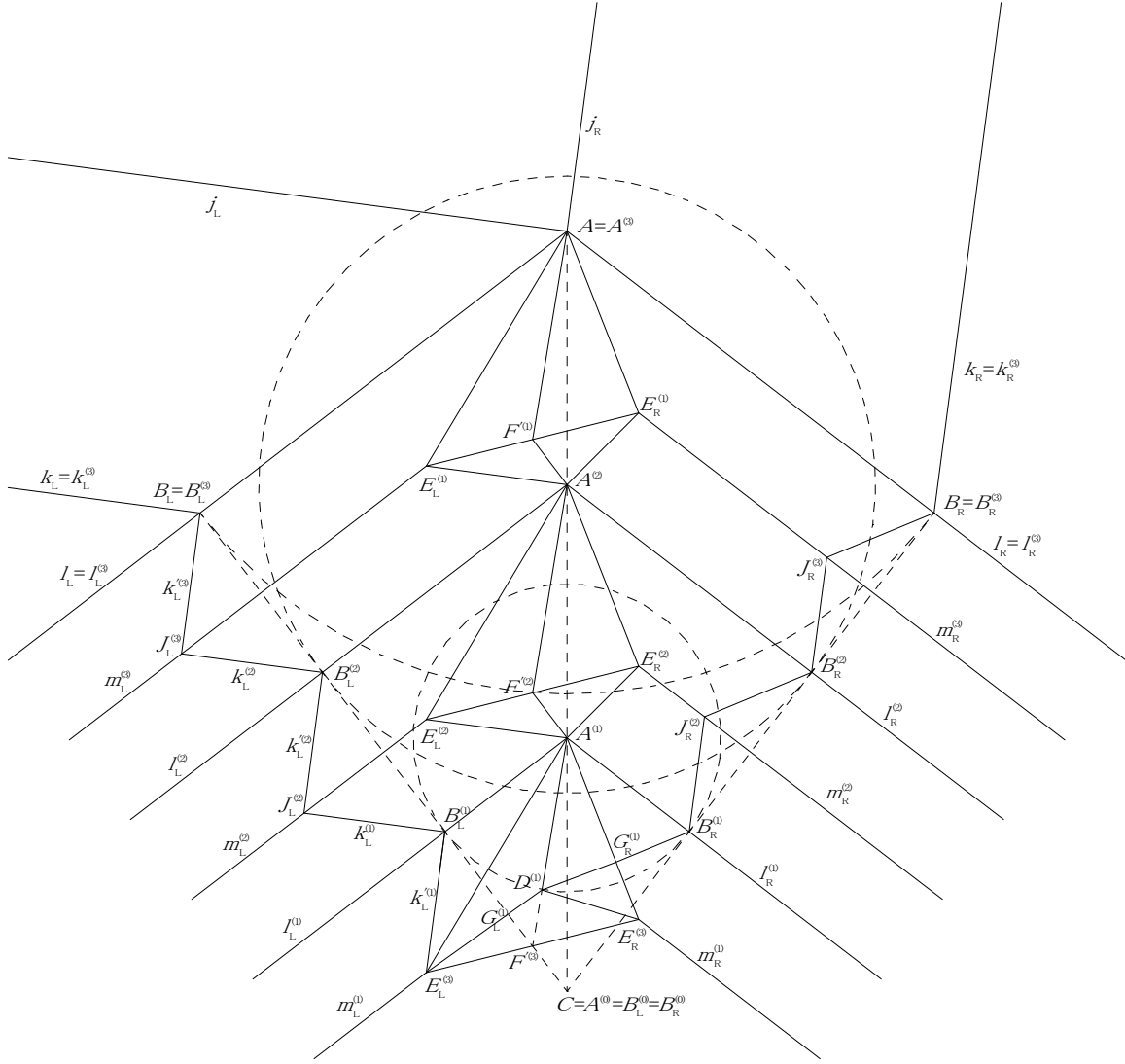


FIGURE 7.10. Simpler CP of the division of our improved 3D gadgets

Proposition 7.11. *Suppose $\phi_\sigma/2 = \zeta_\sigma$ in Construction 7.1. If $D^{(n)}$ and $D^{(n-1)}$ exist in (8), then $K_\sigma^{(n)}$ given in (9) and $M_\sigma^{(n)}$ given in (10) are identical points.*

Thus from Propositions 7.7, 7.8 and 7.11, we obtain Table 7.12 which gives the assignment of mountain folds and valley folds in the case of $\phi_\sigma/2 = \zeta_\sigma$ in the resulting crease pattern in Construction 7.1.

8. CONCLUSION

In this paper we presented a construction of flat-back 3D gadgets completely downward compatible with the conventional pyramid-supported ones. Since there are an infinite number of gadgets

	common creases	n with $2 \leq n \leq d$ such that	
		$\exists D^{(n)}$	$\nexists D^{(n)}$
mountain	$j_\sigma, \ell_\sigma^{(n)}, A^{(1)} D^{(1)},$	$A^{(n-1)} E_\sigma^{(n)}, B_\sigma^{(n)} J_\sigma^{(n)}$	
folds	$B_\sigma^{(1)} E_\sigma^{(1)}, D^{(1)} E_\sigma^{(1)}$	$A^{(n)} D^{(n)}, D^{(n)} K_\sigma^{(n)}$	$A^{(n)} F^{(n)}$
valley	$k_\sigma, m_\sigma^{(n)},$	$B_\sigma^{(n-1)} J_\sigma^{(n)}$	
folds	$A^{(n)} E_\sigma^{(n)}, E_L^{(n)} E_R^{(n)}$	$A^{(n-1)} D'^{(n-1)}, D'^{(n)} K_\sigma^{(n)}$	$A^{(n-1)} F^{(n)}$

TABLE 7.12. Assignment of mountain folds and valley folds for the division of the new gadget for $\phi_\sigma/2 = \zeta_\sigma$

parametrized by ϕ_σ or ψ_σ compatible with a given conventional gadget, we face a new problem of what choice of gadget suits our requirements. We suggested some choices of typical gadgets, that is, critical, orthogonal and balanced gadgets to design the crease pattern as easy to fold as possible. For a similar purpose, we also presented a construction of our 3D gadgets specifying ϵ_σ instead of ϕ_σ or ψ_σ . On the other hand, problems such as maximizing the height of an extrusion which we considered in Example 6.9 may only be solved computationally.

Although our improved 3D gadgets have the complete downward compatibility with the conventional ones in addition to the advantages mentioned in the introduction, our 3D gadgets have one definite disadvantage that they need to fold more creases than the conventional ones, which makes the folding a little more complicated and time-consuming even if we make a good choice of gadgets. Thus when we design and make an origami extrusion, it will be still useful to make prototypes with the conventional gadgets, while we can use our improved gadgets in a finishing work by replacing the conventional ones.

In this paper we did not mention negative 3D gadgets, which we gave two constructions for our previous 3D gadgets in [1], Section 9. However, negative gadgets for our improved gadgets are also of our concern, and will be treated in a sequel to this paper since we need a little more preparation for introducing a third construction.

It may be time to give a name to our 3D gadgets to distinguish them from the conventional pyramid-supported ones. Let us call our flat-back 3D gadgets constructed in the previous and the present paper *origon gadgets* or simply *origons*, which is a coined word combining ‘origami’ and ‘polygon’ or suffix ‘-on’ (meaning a fundamental unit in high energy physics, molecular biology etc. such as photon and codon). We expect that origon gadgets contribute to future developments of origami extrusions on the basis of our studies.

REFERENCES

- [1] Mamoru Doi, New efficient flat-back 3D gadgets in origami extrusions compatible with the conventional pyramid-supported 3D gadgets, arXiv:cs.CG/1908.07342.
- [2] Toshikazu Kawasaki, On the Relation Between Mountain-Creases and Valley-Creases of a Flat Origami, *Proceedings of the 1st International Meeting on Origami Science and Technology* (Ed. H. Huzita), Ferrara, Italy, 229–237, 1989.
- [3] Carlos Natan Lopéz Nazario, Origami 3D tessellations, *Carlos Natan Lopéz Nazario's photostream at flickr.com*, <http://www.flickr.com/photos/origamiz/sets/72157606559615966/>, 2010.

11-9-302 YUMOTO-CHO, TAKARAZUKA, HYOGO 665-0003, JAPAN
E-mail address: doi.mamoru@gmail.com